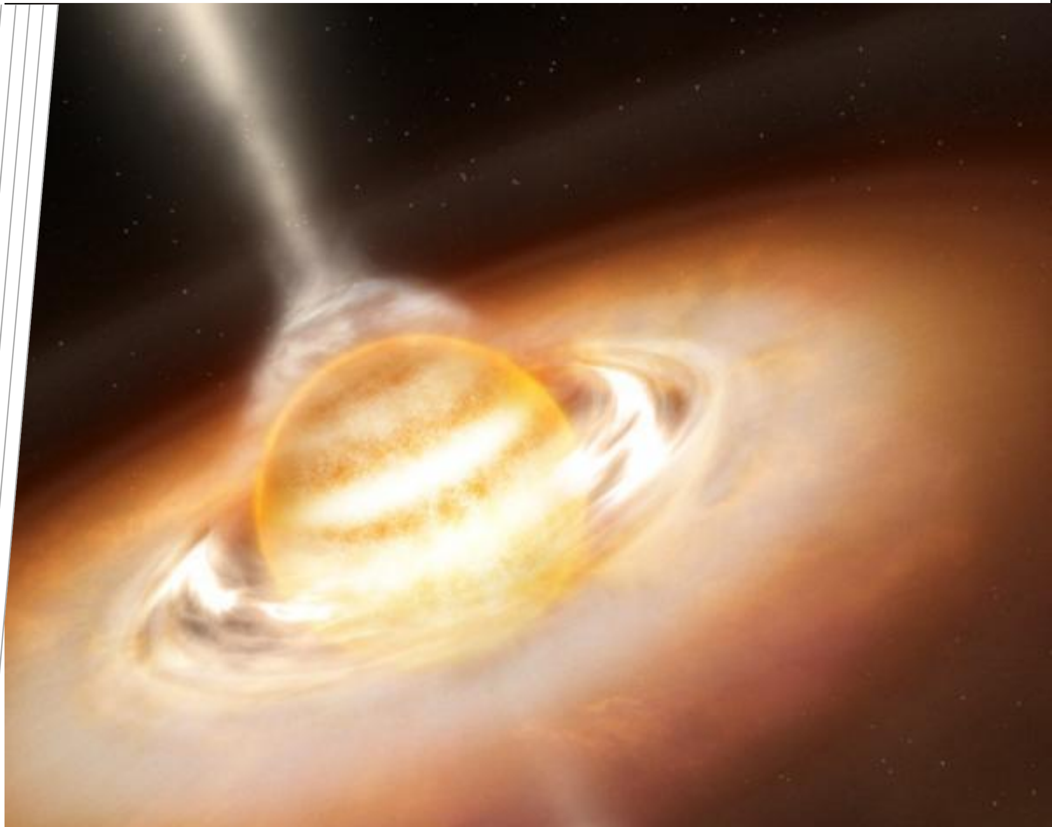

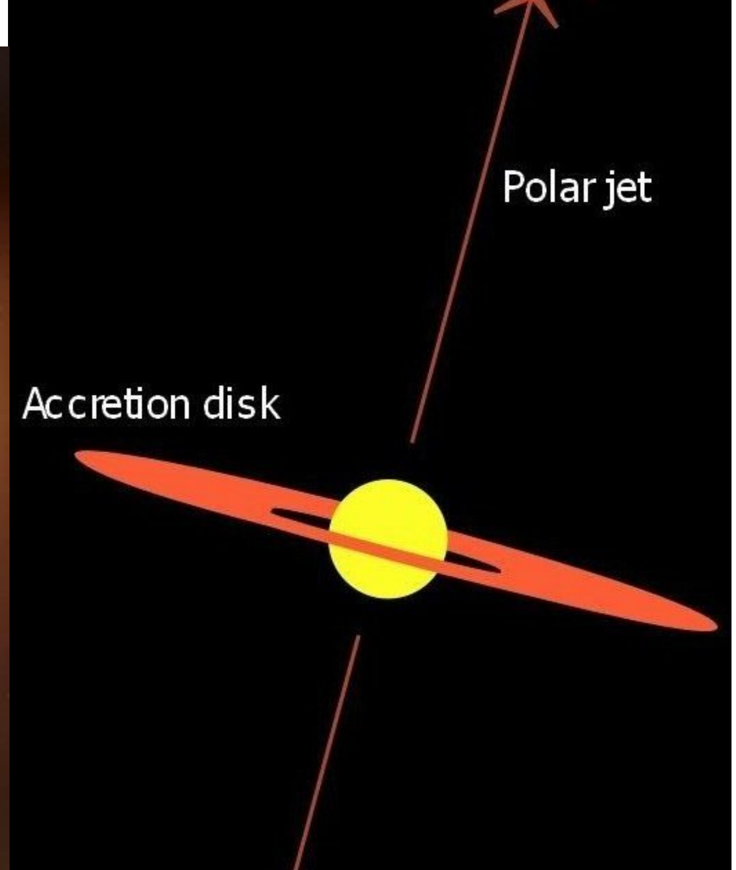

www.csiro.au

Magnetic pressure driven jet flow in young stellar systems

Kurt Liffman, CSIRO and Swinburne University of Technology

Acknowledgement: ATNF/CASS Astrophysics Group

Cosmic Magnetism Conference; 8th June 2010

CSIRO

Meteorites: Foundation Stones of the Planets

Cross section of the Allende carbonaceous chondrite

Chondrules formed ~ million years after CAIs

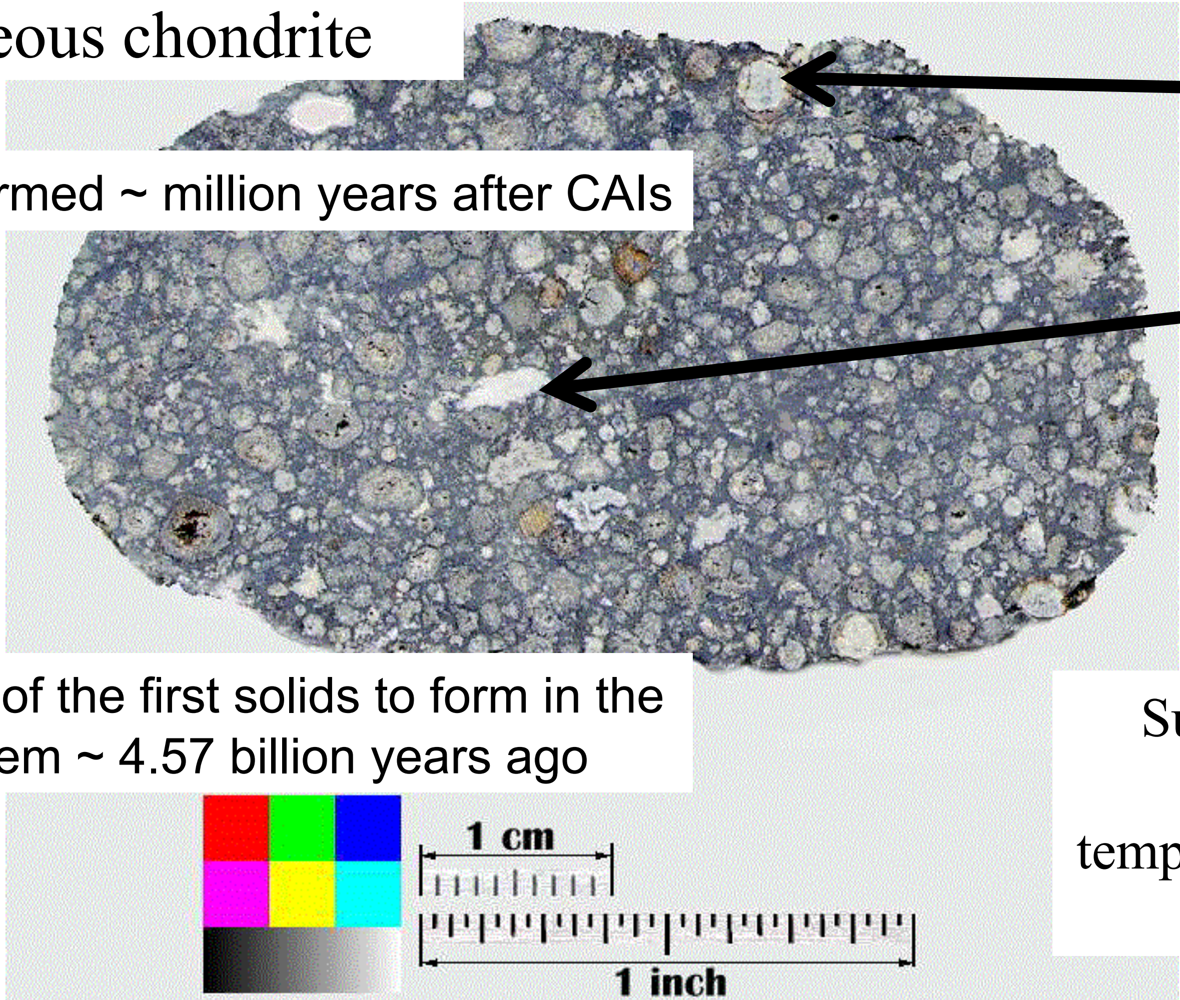

Chondrules
(melt objects)
1800 K

Calcium Aluminium Inclusion (CAI)
(condensates)
2000 K

CAIs – some of the first solids to form in the solar system ~ 4.57 billion years ago

Surrounding matrix (contains high temperature condensates)
500 K

Igneous rocks surrounded by "cold" sedimentary material.
"Hot" rocks surrounded by "cold" material

Formation: local or non-local process?

Chondrules – first noted in 1802; first formation theory in 1877
approximately 20 formation theories developed since 1877

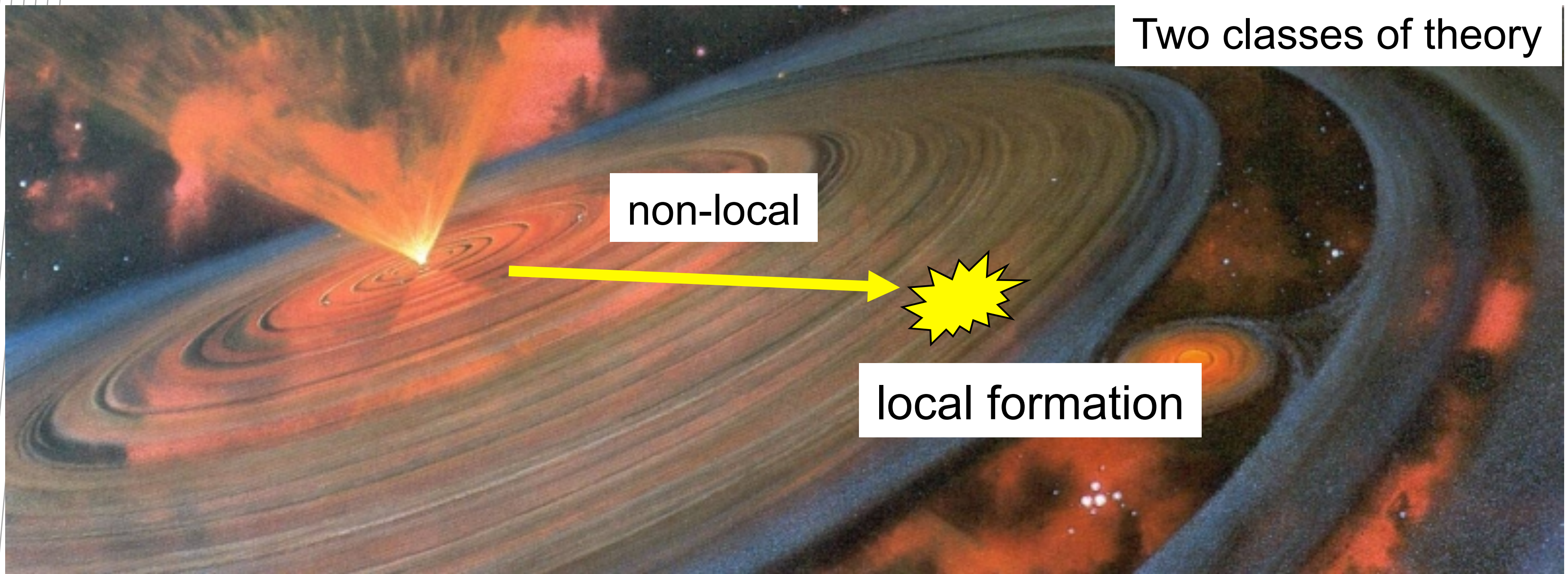

Meteoriticists – various lines of evidence (e.g. meteorites are from the asteroid belt: ~ 3 AU from the Sun) suggest **local** formation

Astrophysicists – most energy at or near the inner rim of the disk: **non-local**

What is the Jet Flow Model?

Skinner (1990), Liffman (1991/2), Cameron (1994), Liffman & Brown (1995/6), Shu et al. (1996)

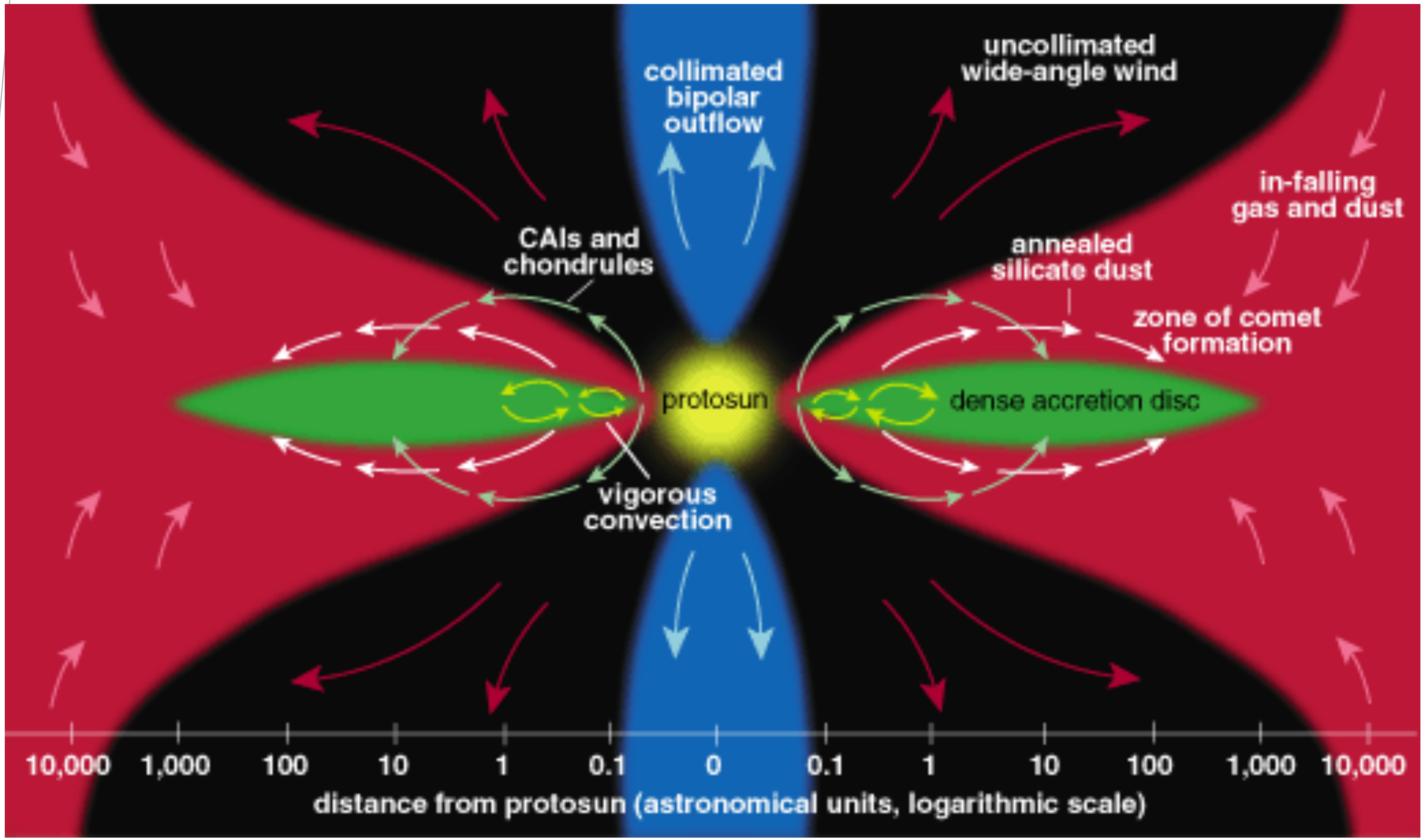

Nuth III J. A., 2001 American Scientist, **89**, 228-235

Jet Processing of an Accretion Disk

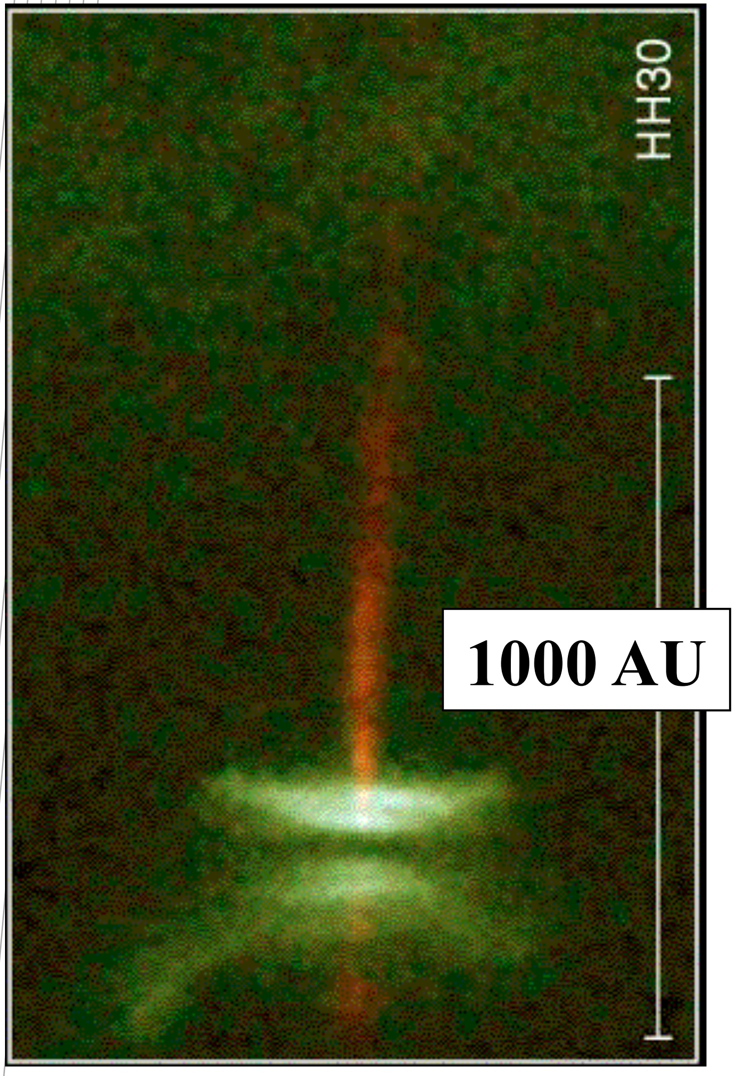

- Lifetime 10^6- 10^7 years
- Lifetime outflow mass ejected ≈ 0.1 $M_\odot$
- outflow "rock" mass ejected 10^{-3} - 10^{-4} $M_\odot$
- Total rock mass of the planets ≈ 10^{-4} $M_\odot$

10% fall back implies 10^{-4} - 10^{-5} $M_\odot$ returned to the solar nebula

Predictive Theory:
Chondrules/CAI formed over a 10^7 year period. (Liffman 1992)
Chondrules/CAI to be found in comets (Skinner 1990, Liffman, Shu et al.)

CSIRO

Stardust Mission

Dust particles obtained from a Kuiper Belt (i.e. ~ 40 AU) comet

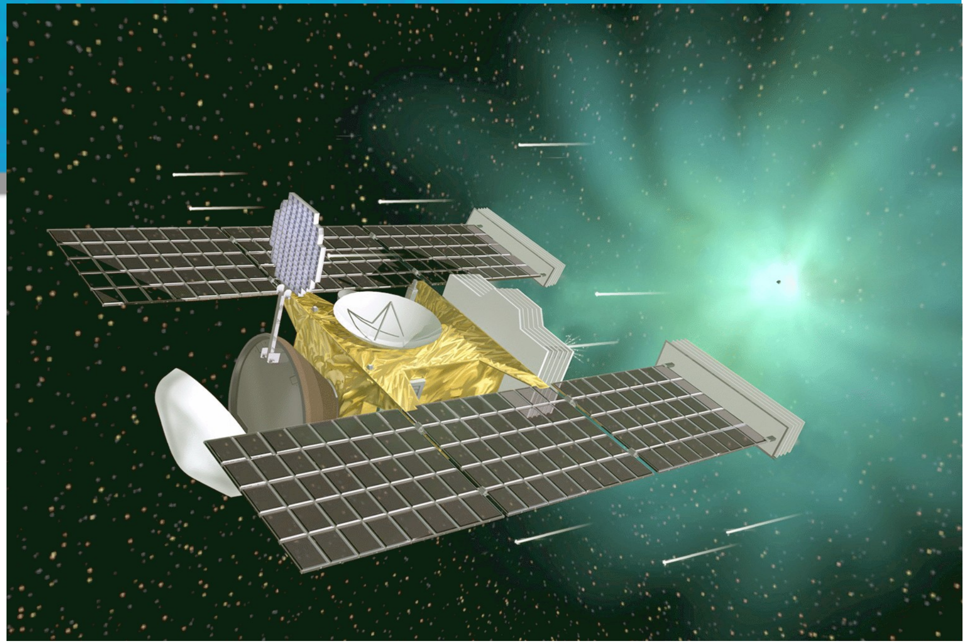

Brownlee et al. (2006)

Same pattern as seen in meteorites: High formation temperature (> 1400K) rocks surrounded by cold material – in this case, ice.

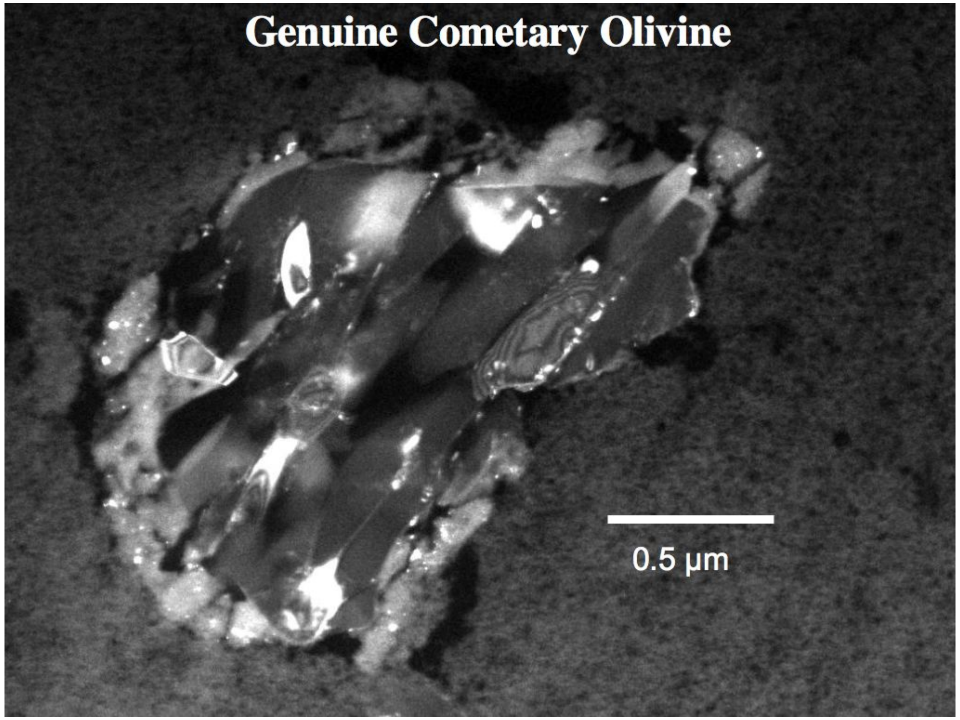

Chondrules and CAIs also found in Comet Wild 2

Nakamura et al. (2008)

strongly suggest non-local formation. At 40 AU high temperature heating is difficult to understand

Observations - forsterite dust formed in the interior disk regions surrounding Sun-like stars

Abraham et al. Nature 2009

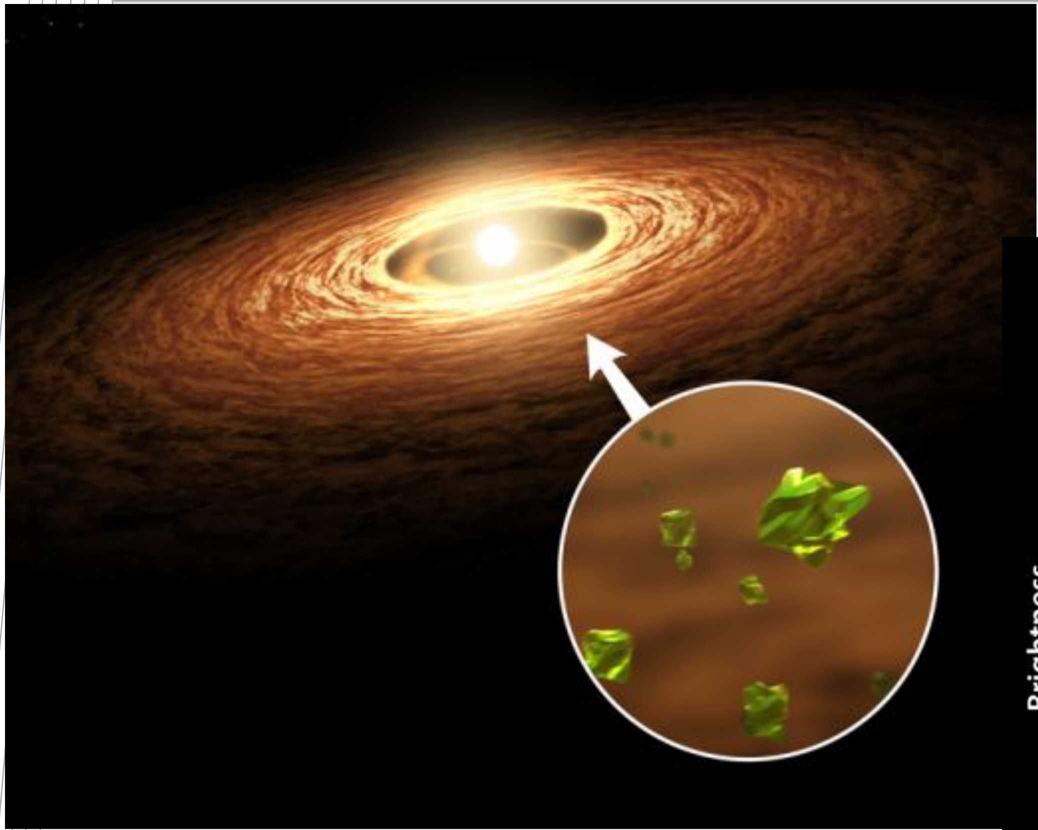

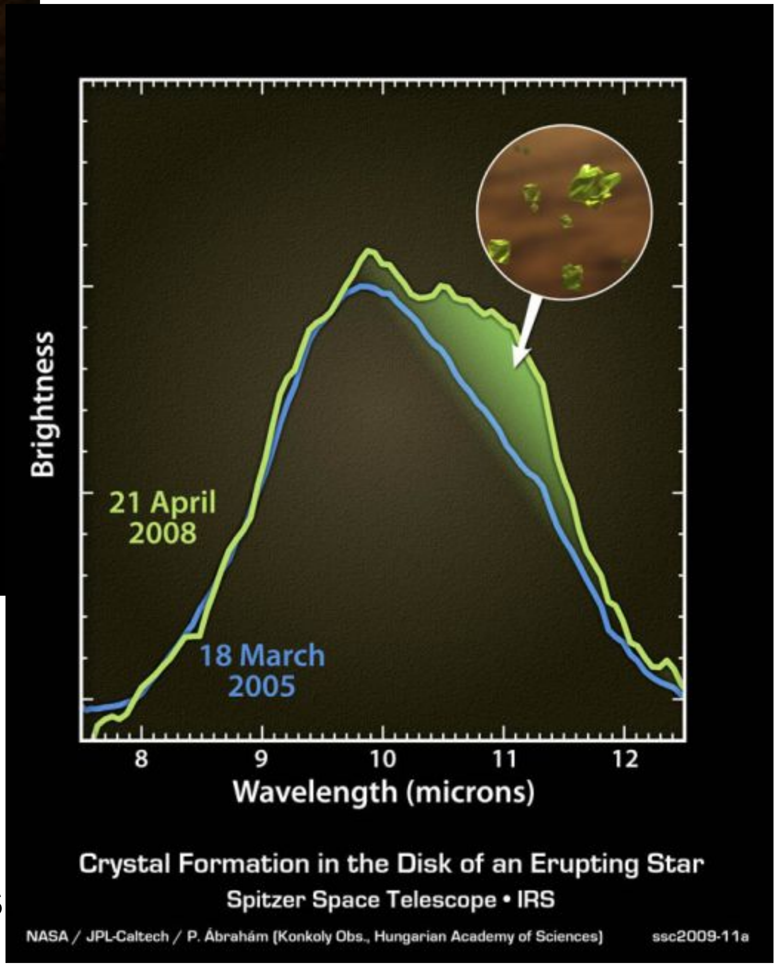

“star burst” produces forsterite (Mg_2SiO_4) grains from amorphous dust within or around ~ 0.5 AU from the star

These type of grains are observed in comets
Non-local formation!

“Modelling” the Jet Model – Inner Disk

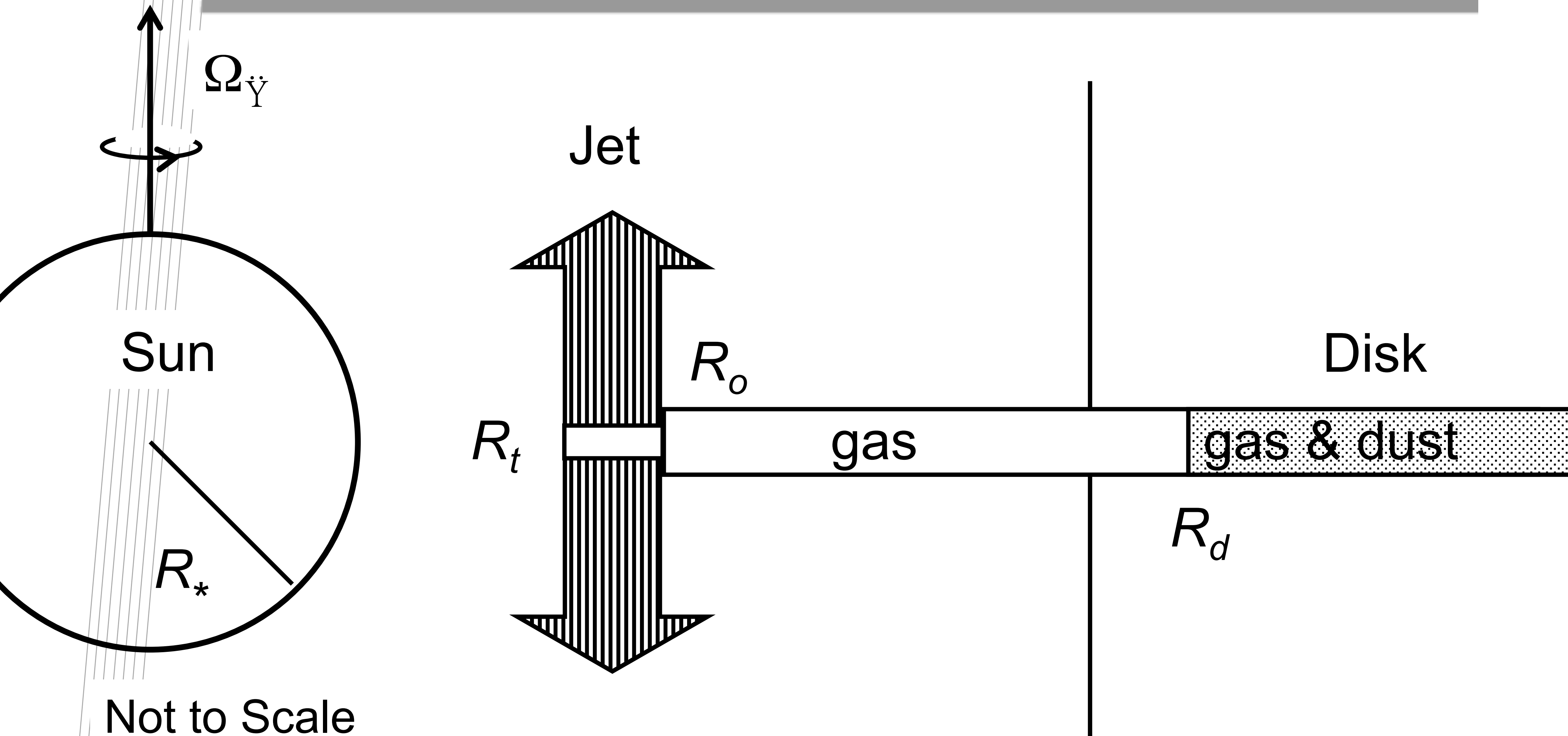

What is the jet flow mechanism?

Will consider magnetic pressure, instead of centrifugally driven

Protostellar/T Tauri Jets

Two basic models:

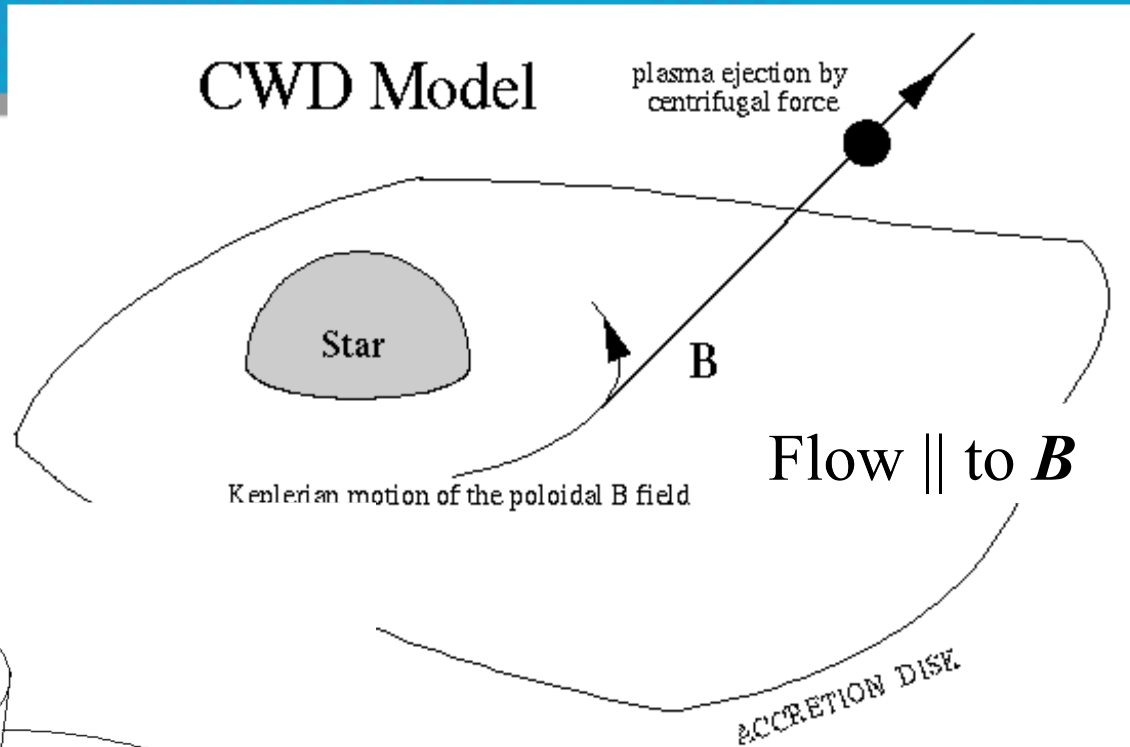

Flow || to ***B***

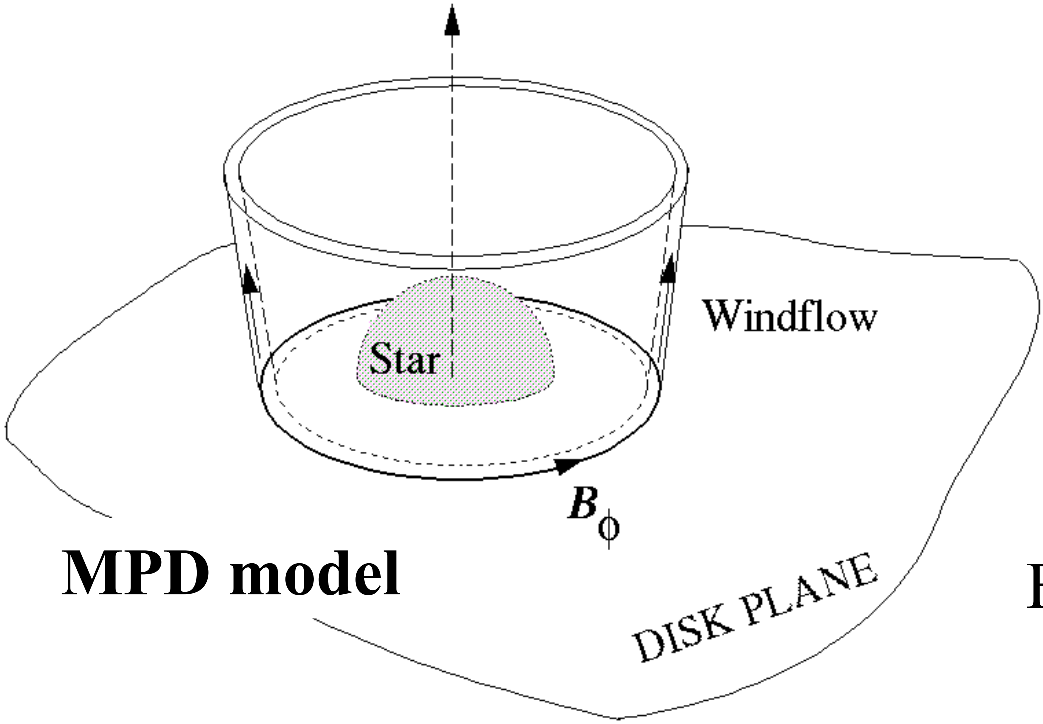

MPD model

Why the dichotomy?

Flow ⊥ to ***B***

Star-Disk Electric Circuit – J, B, E

Relative motion between the disk and stellar magnetic field generates an electric field

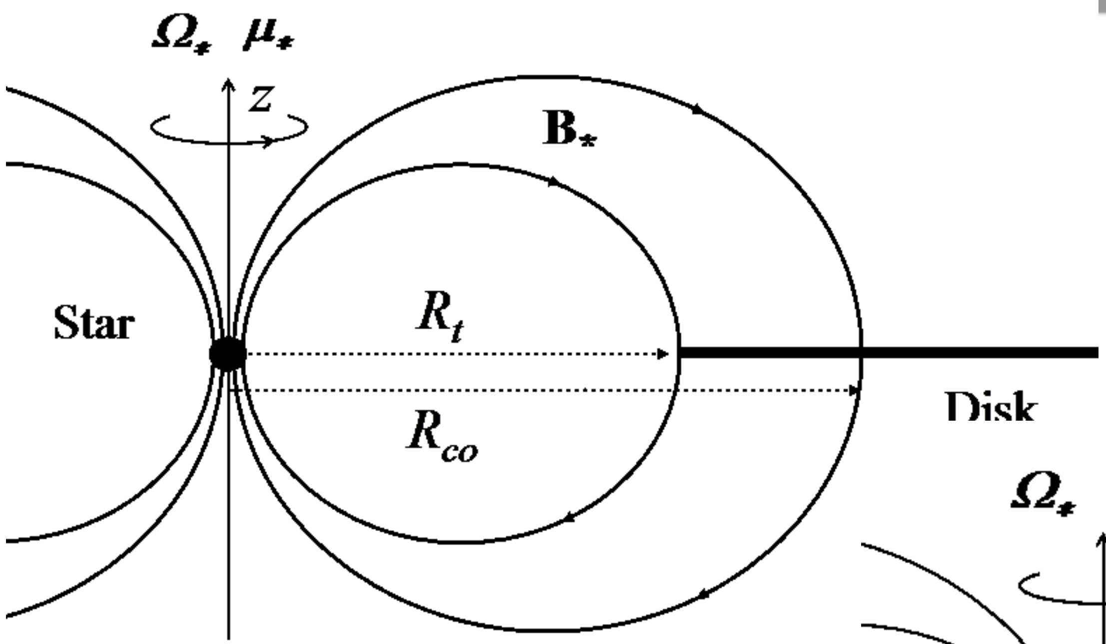

R_t – truncation radius
R_{co} – co-rotation radius
B_* - stellar magnetic field
j – current density

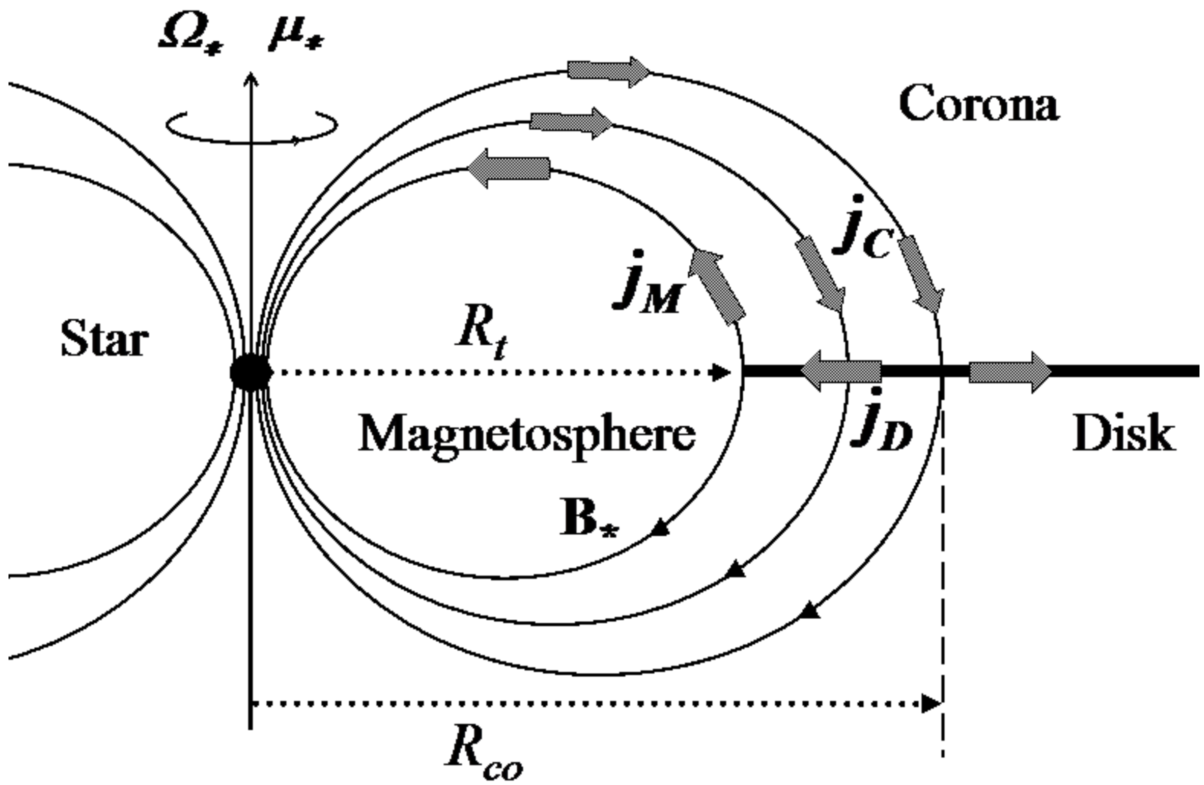

Nothing wrong with the MHD description, but the J, B, E description may provide some different insights.

Star-Disk Electric Circuit

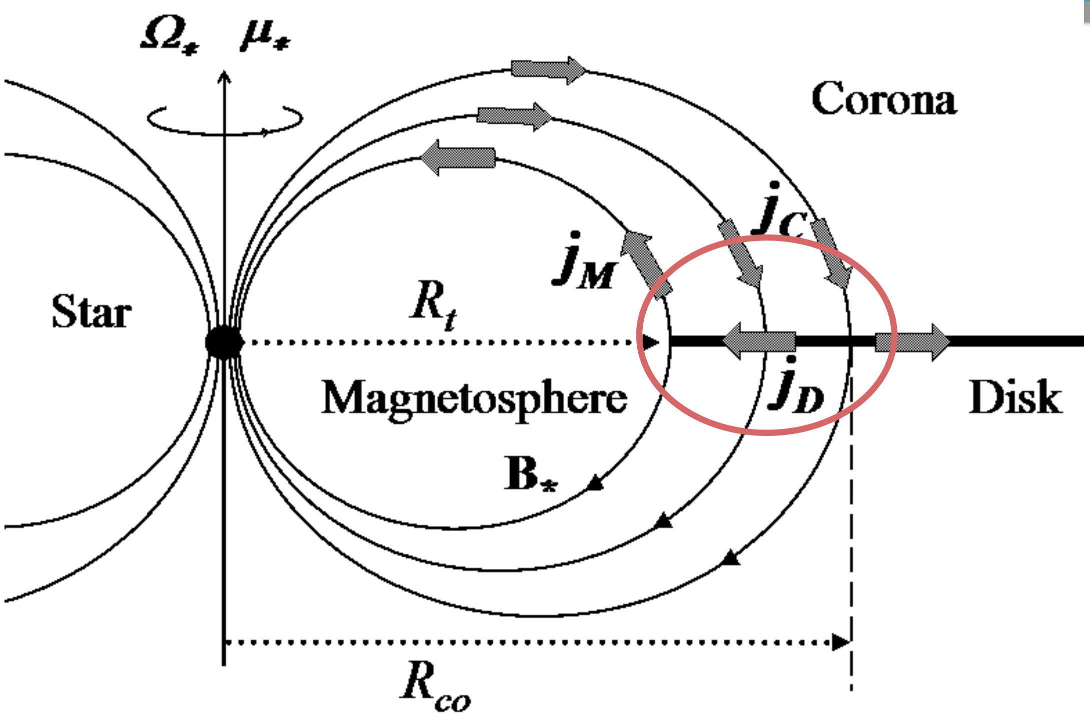

Toroidal magnetic field induced within the disk

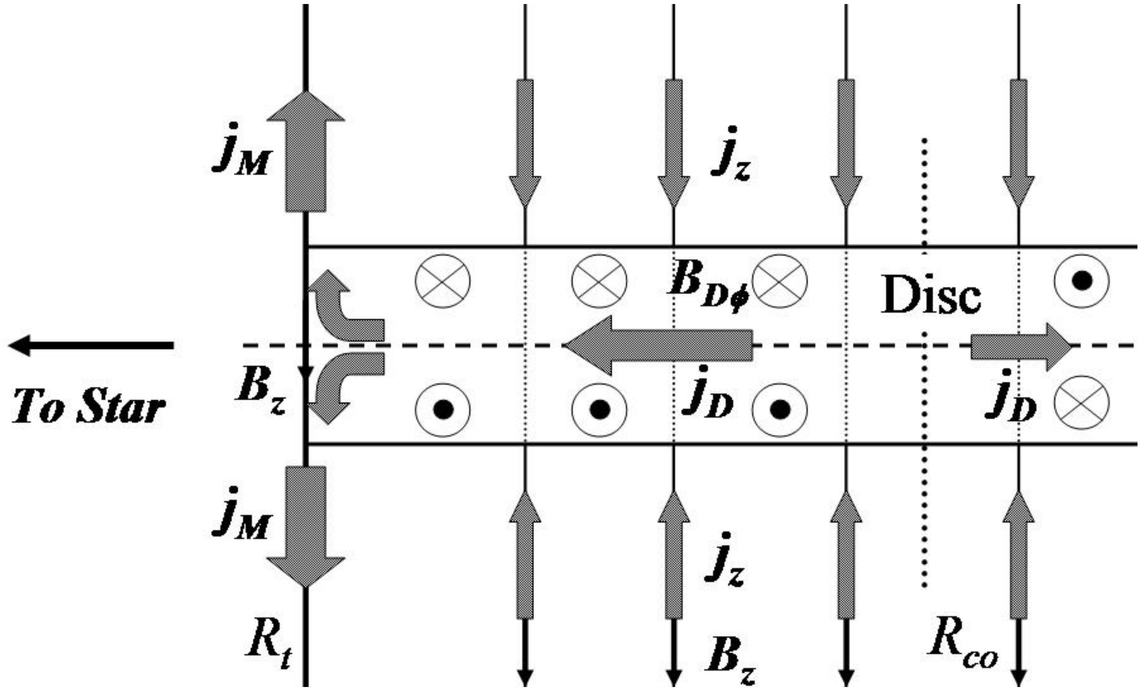

Magnetic Scale Height

The z component of the steady state momentum equation

$$\rho(\mathbf{v} \bullet \nabla)\mathbf{v} = -\nabla p + \rho\mathbf{g} + \mathbf{j} \times \mathbf{B}$$

hydrostatic ($\mathbf{v} = \mathbf{0}$), isothermal form: $$\frac{\partial \rho}{\partial z} + \chi z \rho + \xi z = 0$$

which has the solution

$$\rho(r,z) = \rho_c(r)\exp\left[-\left(\frac{z}{h}\right)^2\right] - \rho_\infty\left(1 - \exp\left[-\left(\frac{z}{h}\right)^2\right]\right)$$

where

$$\rho_\infty = (\mu_0 \sigma r)^2 \left(\frac{B_z^2}{\mu_0}\right)\left(\frac{\Omega_*}{\Omega_K} - 1\right)^2$$

Magnetic Scale Height

For the magnetically confined disk there is a distance from the central plane of the disk, H_B, where the density of the disk goes to zero

$$\rho(r,z) = 0 \Rightarrow z = H_B = h\sqrt{\ln\left[1 + \frac{\rho_c(r)}{\rho_\infty}\right]}$$

Although this is the true height of the disk, it has a problem:

$$B_z \to 0 \Rightarrow \rho_\infty \to 0 \Rightarrow H_B \to \infty$$

A more consistent definition gives the e-folding magnetic scale height, h_B.

$$\rho(r,z) = \frac{\rho_c}{e} \Rightarrow h_B = h\sqrt{\ln\left[1 + \frac{1 - 1/e}{1/e + \rho_\infty / \rho_c(r)}\right]}$$

Which has the desired property that $B_z \to 0 \Rightarrow h_B \to h$

CSIRO

Example: X-ray Binary

$$\sigma = \frac{1}{\mu_0 \eta_*} \approx \frac{1}{\mu_0 \nu_*}$$

$r_* = 10^4$ m

$M_* = \mathrm{M_{sol}}$

$\dot{M} = 10^{-8}\ \mathrm{M_{sol}}$ / yr

$\mathrm{r_c} = 2r_*$

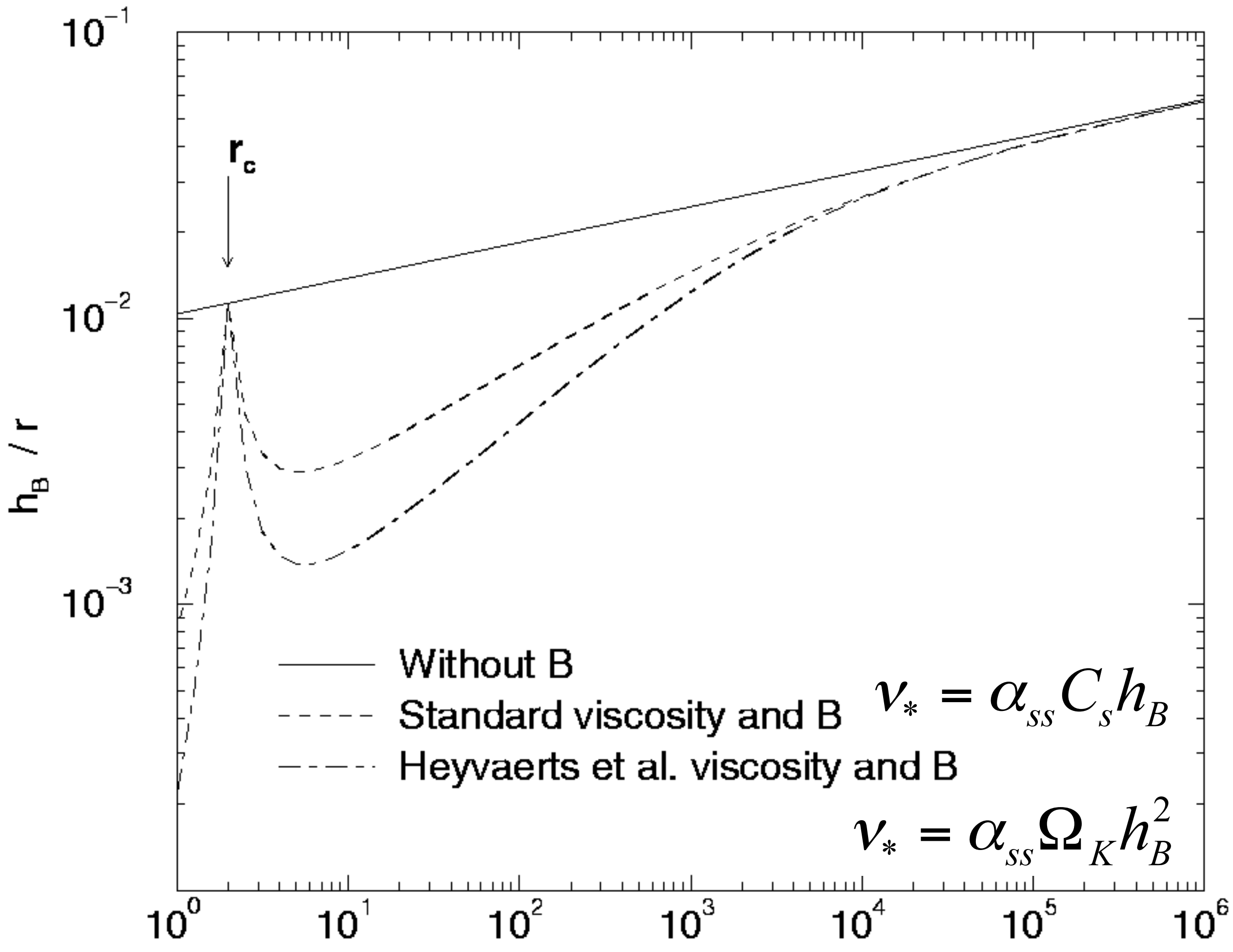

$$\nu_* = \alpha_{ss} C_s h_B$$

$$\nu_* = \alpha_{ss} \Omega_K h_B^2$$

$$r / r_*$$

Liffman and Bardou (1999)

Star-Disk Torque

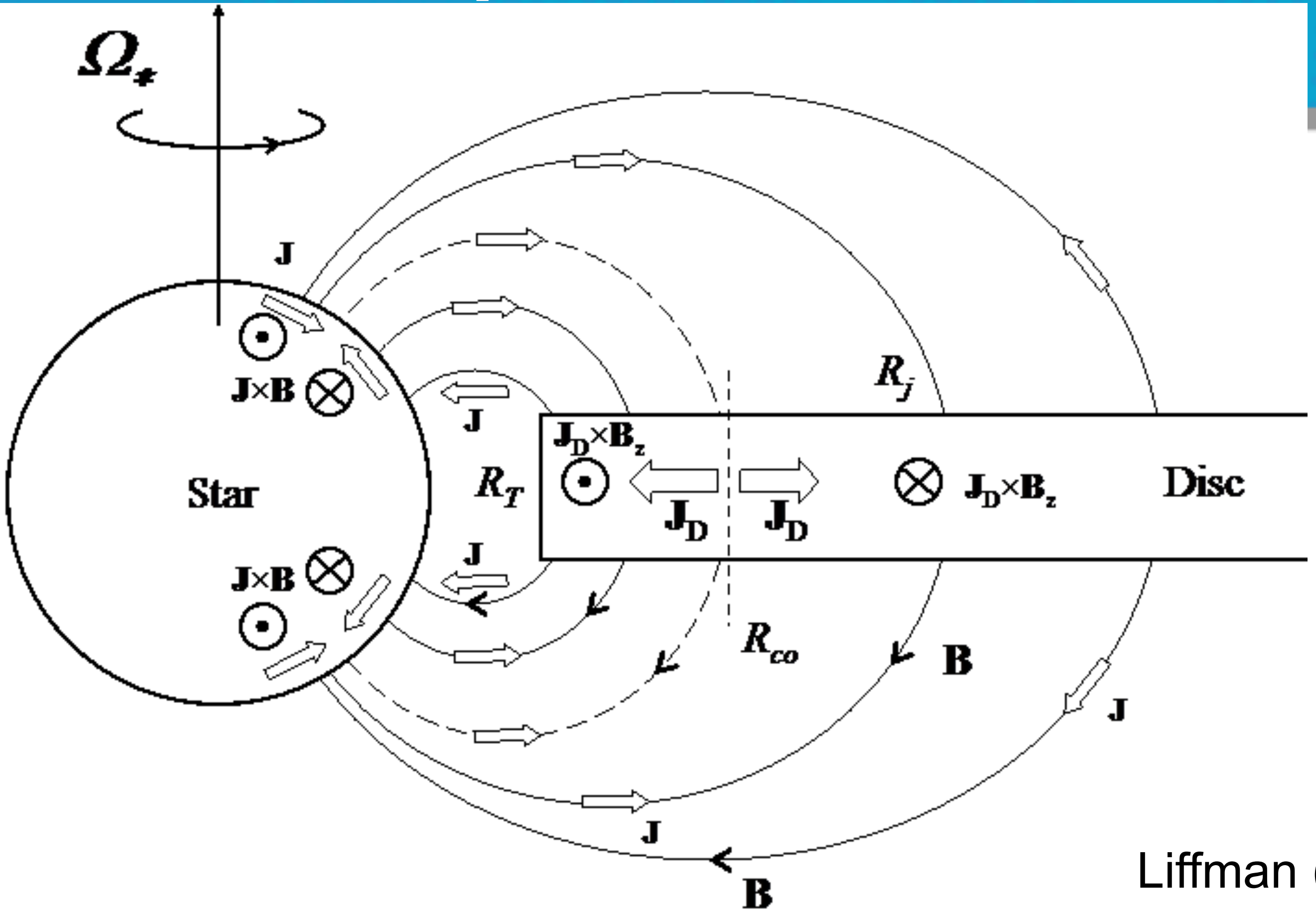

Liffman (2007)

The *J*, *B*, *E* model - same as the MHD answer for the torque on the disk from the star

$$\frac{d\tau}{dr} = \frac{4\pi r^2 B_\phi B_{*z}}{\mu_0}$$

Suppose there is a trans-field, short-circuit – perhaps due to Gravity Drift

Gravitational Drift

Gravitational Drift drives a radial current that short circuits the star-disk current

$$\mathbf{V}_D = \frac{\mathbf{F}_\perp \times \mathbf{B}}{qB^2}$$

Drift Velocity

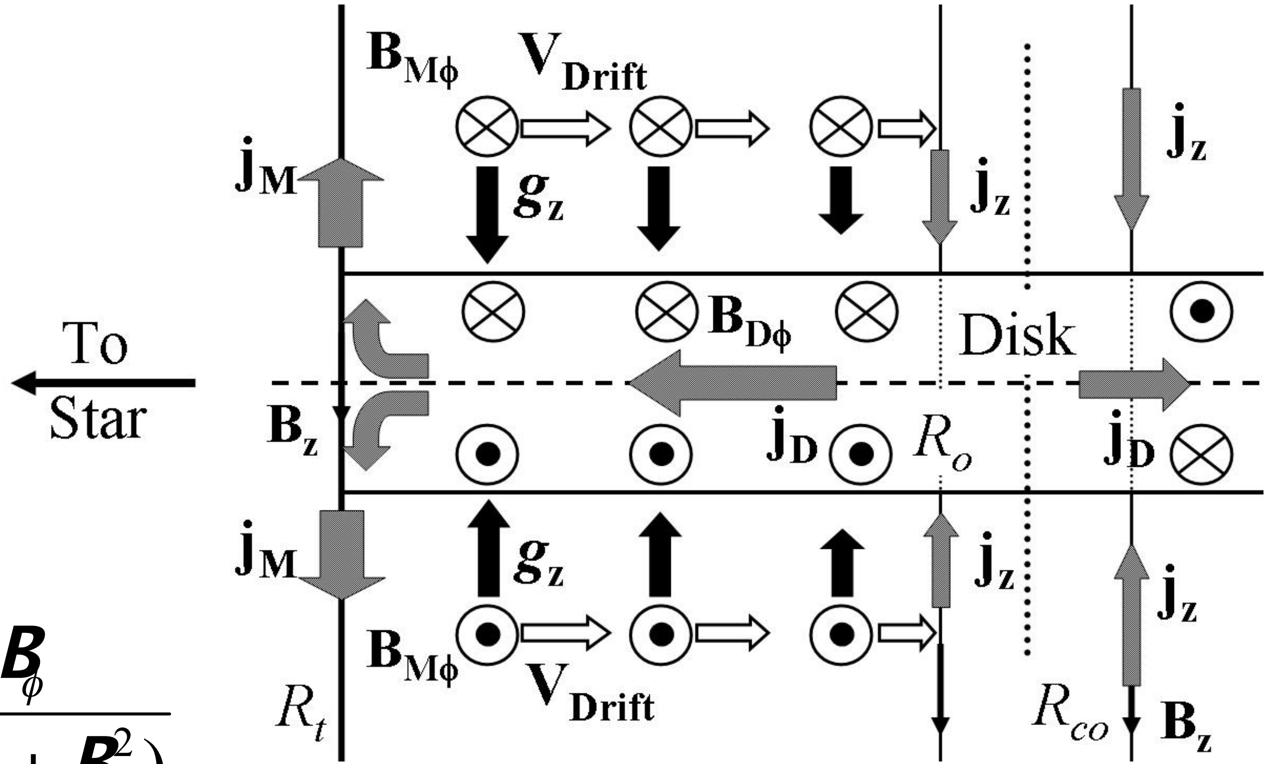

Liffman (2007)

$$j_{\perp r} \approx \frac{n_i G M m_i z B_\phi}{(r^2+z^2)^{3/2}(B_\phi^2+B_z^2)}$$

Gravitational Drift Current

Short-Circuit – Toroidal Field

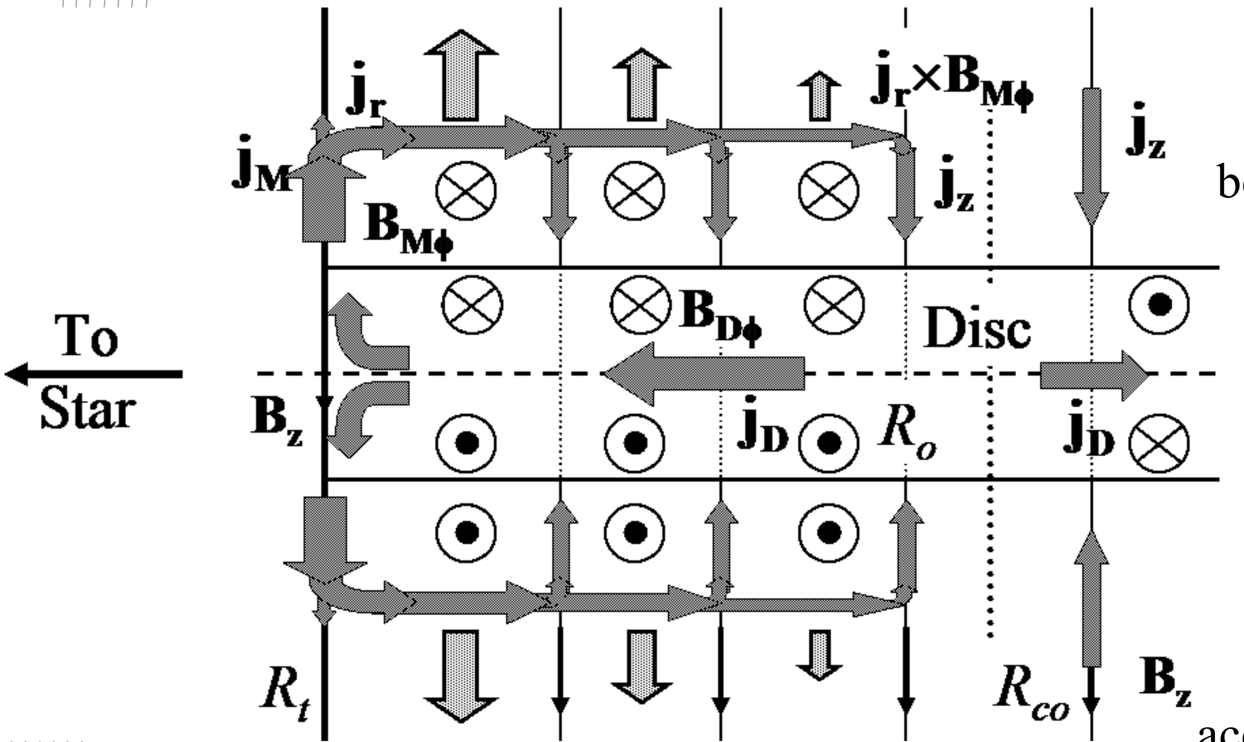

The radial transfield currents produce toroidal fields above and below the disk. $j \times B$ flow points away from the disk.

acceleration region starts near the top of the disk ($z = z_0$)

acceleration region finishes when the radial current is exhausted ($z = z_T$)

Assume $\mathbf{j}_r$ is a constant with z

toroidal field

$$B_\phi(r,z) = \frac{\mu_0 I_r(r)}{2\pi r_0}\left(1 - \frac{z - z_0}{z_T - z_0}\right) = 2.7 \times 10^{-4}\,\frac{\left(I_r / 10^{13}\,\mathrm{A}\right)}{\left(r/0.05\mathrm{AU}\right)}\left(1 - \frac{z - z_0}{z_T - z_0}\right)\mathrm{T}$$

Liffman (2007)

Short Circuit – Total Force

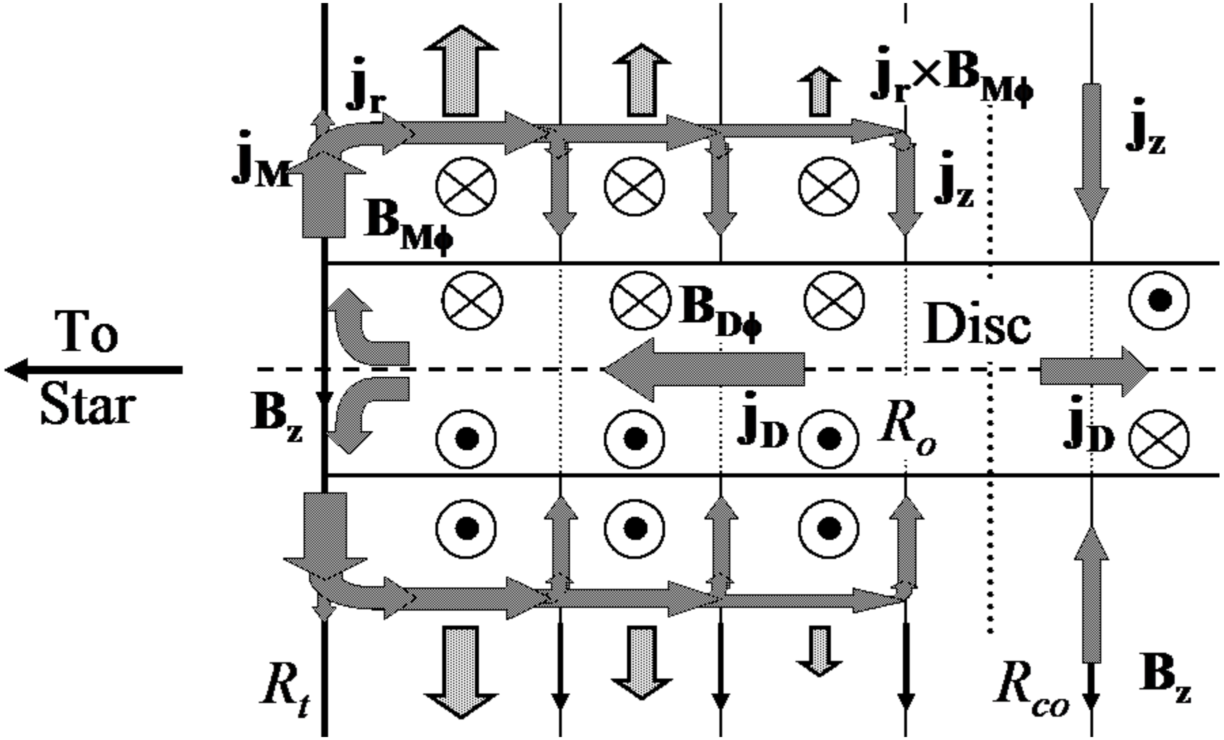

Integrate $j_r \times B_\phi$ over volume – total force is independent of j_r variation with z

$$\boldsymbol{F} = \frac{\mu_0 \boldsymbol{I_M I_r}}{4\pi} \ln\left(\frac{\boldsymbol{r_o}}{\boldsymbol{r_i}}\right)\left(2 - \frac{\boldsymbol{I_r}}{\boldsymbol{I_M}}\right)$$

This implies that the ejection speed of the gas is independent of j_r variation with z

Short-Circuit – Ejection Speed

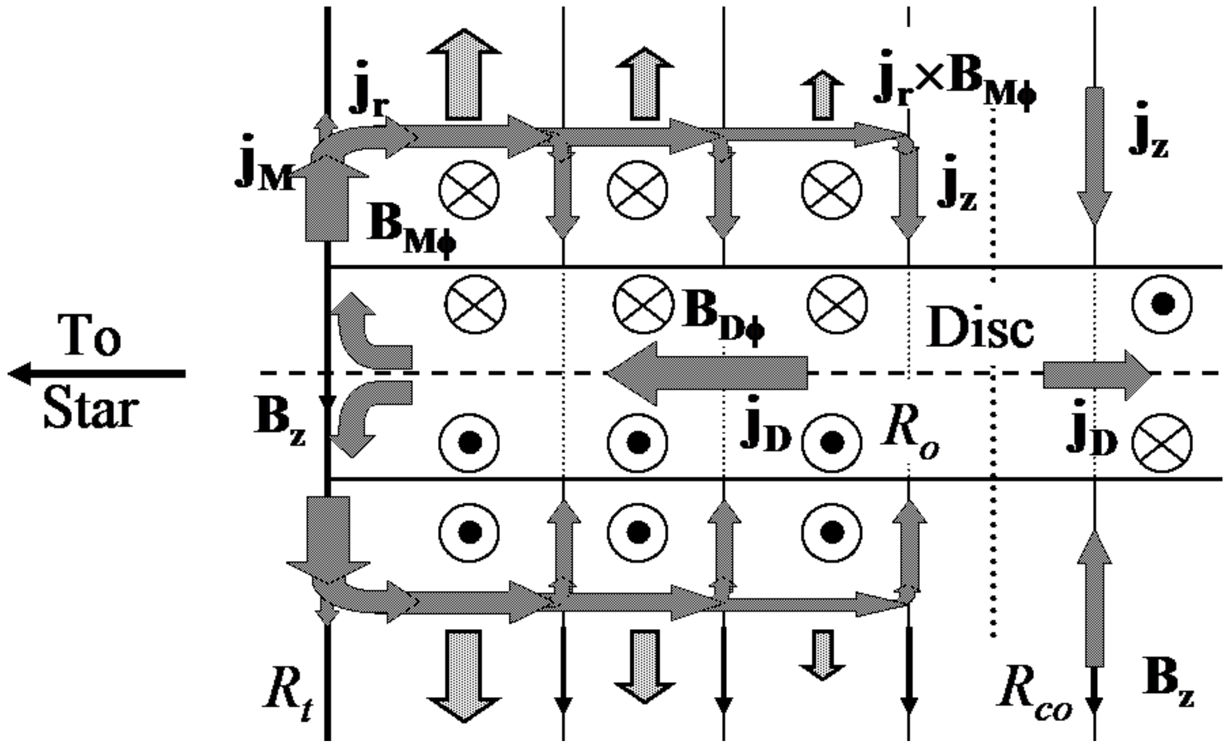

Potentially high exhaust speed

$$v_e \approx \sqrt{\frac{\mu_0}{2\rho_0}} \frac{I_r(r_0)}{\pi r_0} = 337 \sqrt{\frac{10^{-12}\,\mathrm{kg\,m^{-3}}}{\rho_0}} \left(\frac{I_r}{10^{13}\,\mathrm{A}}\right)\left(\frac{0.05\,\mathrm{AU}}{r_0}\right) \mathrm{km\,s^{-1}}$$

Acceleration Region: Flow Speed

The z component of the steady state momentum equation

$$\rho(\mathbf{v} \bullet \nabla)\mathbf{v} = -\nabla p + \rho\mathbf{g} + \mathbf{j} \times \mathbf{B}$$

We can obtain a general flow speed "Bernoulli-like" equation

$$V_z^2(z_T) = V_z^2(z_0) + 2GM\left(\frac{1}{\sqrt{r^2 + z_T^2}} - \frac{1}{\sqrt{r^2 + z_0^2}}\right) + \frac{\mu_0 I_M I_r}{2\pi^2 \rho_0 r_0^2}$$

This allows us to deduce solutions for distance, speed, density of the flow as a function of time

Liffman et al. (2011)

Toroidal Fields?

How can toroidal fields drive the flow? Intuitive model

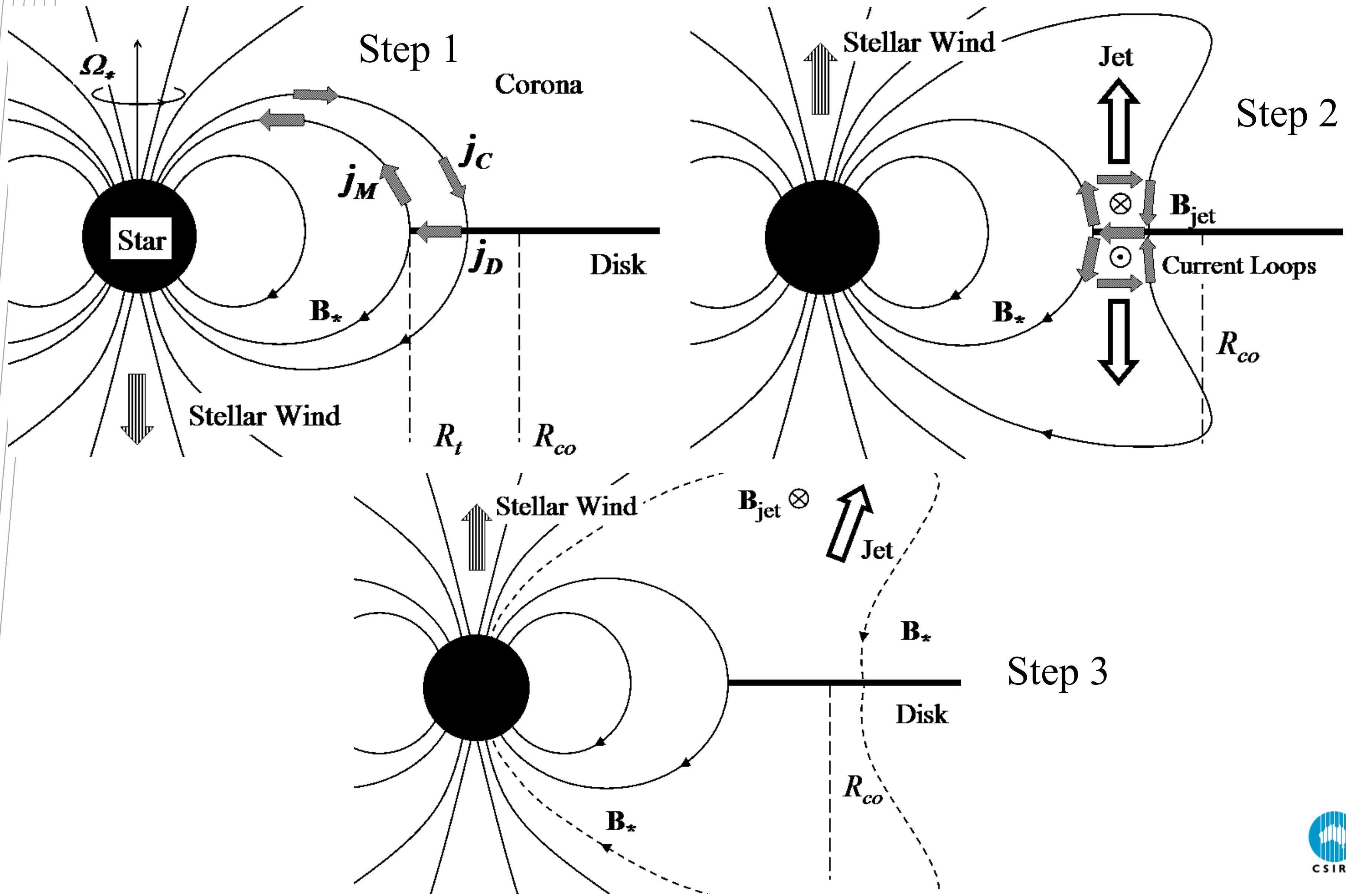

Predictions

This simple theory leads to a number of, potentially, observable predictions

(1) The ejection speed of the flow increases as one approaches the star

$$v_e = \sqrt{\frac{\mu_0}{2\rho_0}\frac{I_r(r_0)}{\pi r_0}} = 337\sqrt{\frac{10^{-12}\,\mathrm{kg\,m^{-3}}}{\rho_0}\left(\frac{I_r}{10^{13}\,\mathrm{A}}\right)\left(\frac{0.05\mathrm{AU}}{r_0}\right)}\ \mathrm{km\,s^{-1}}$$

(2) Stellar rotation period may be a fundamental period of the flow

(3) The flow starts at R_t and ends at "R_o" when the transfield current runs out

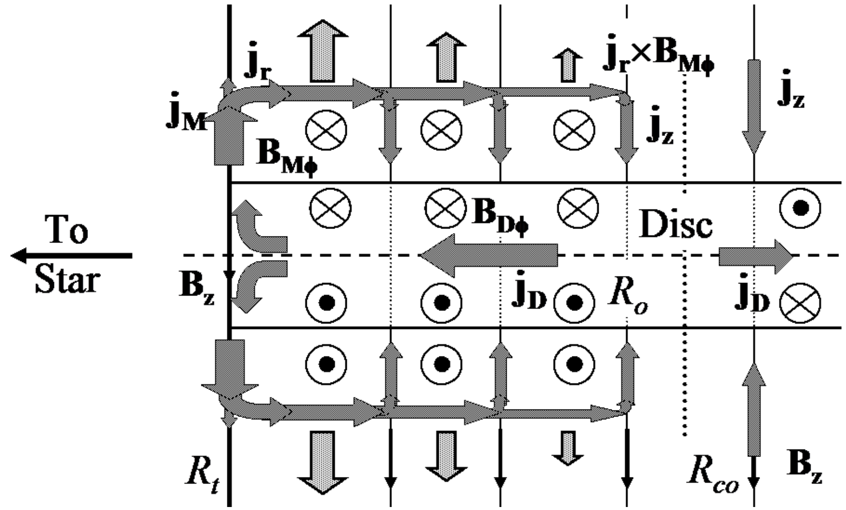

$$\left(\frac{R_t}{R_{co}}\right)^{3/2} - 1 = 2\left(\frac{R_t}{R_{co}}\right)^{3/2}\left(1-\left(\frac{R_t}{R_o}\right)^{1/2}\right) - \frac{5}{4}\left(1-\left(\frac{R_t}{R_o}\right)^2\right)$$

Current balance equation

Predictions

Mass ejection is proportional to mass accretion

$$\dot{M}_w = \frac{\dot{M}_a}{4}\left(\left(\frac{R_o}{R_t}\right)^2 - 1\right)$$

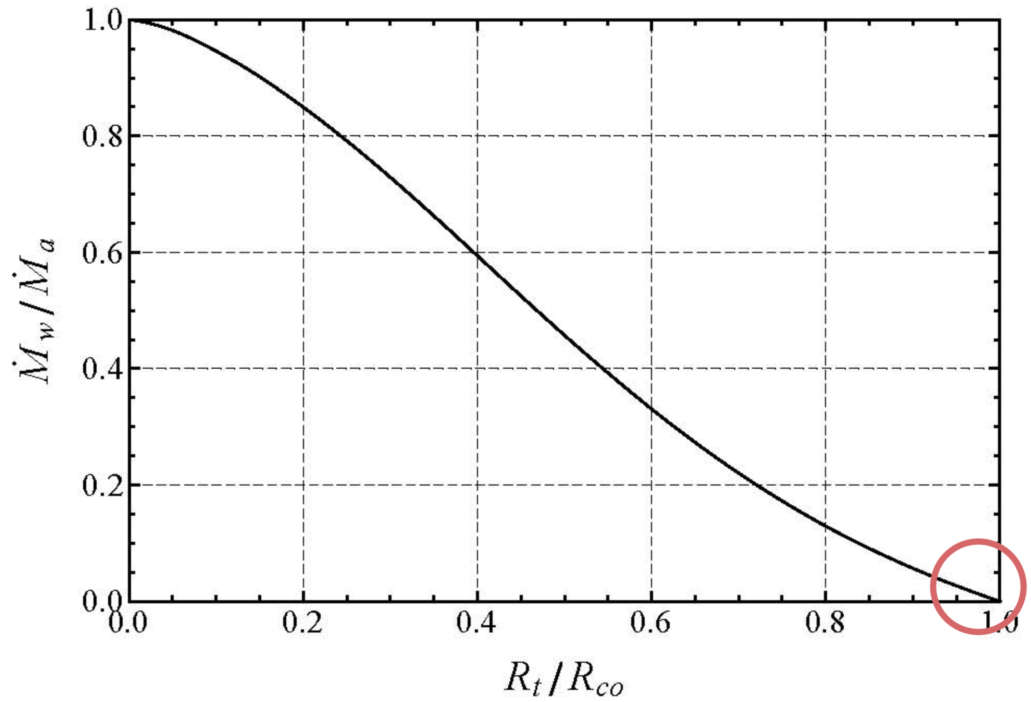

Mass ejection rate and speed increases as the inner edge approaches the star

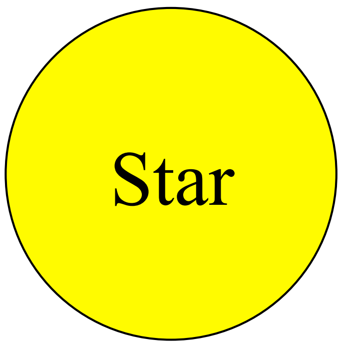

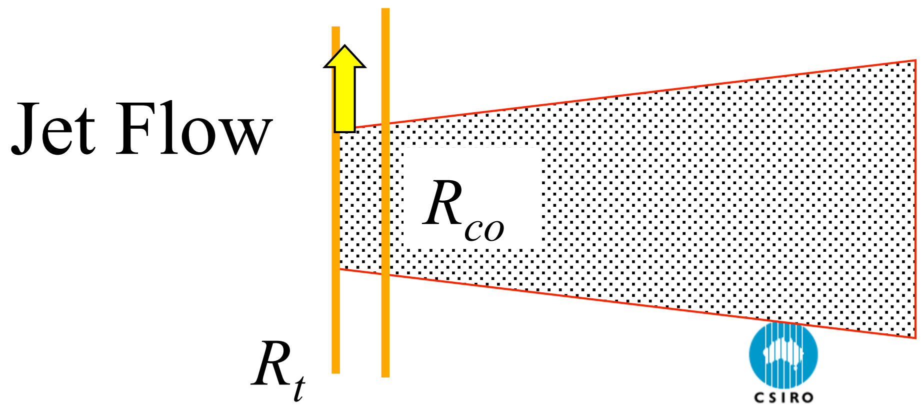

Predictions

Mass ejection is proportional to mass accretion

$$\dot{M}_w = \frac{\dot{M}_a}{4}\left(\left(\frac{R_o}{R_t}\right)^2 - 1\right)$$

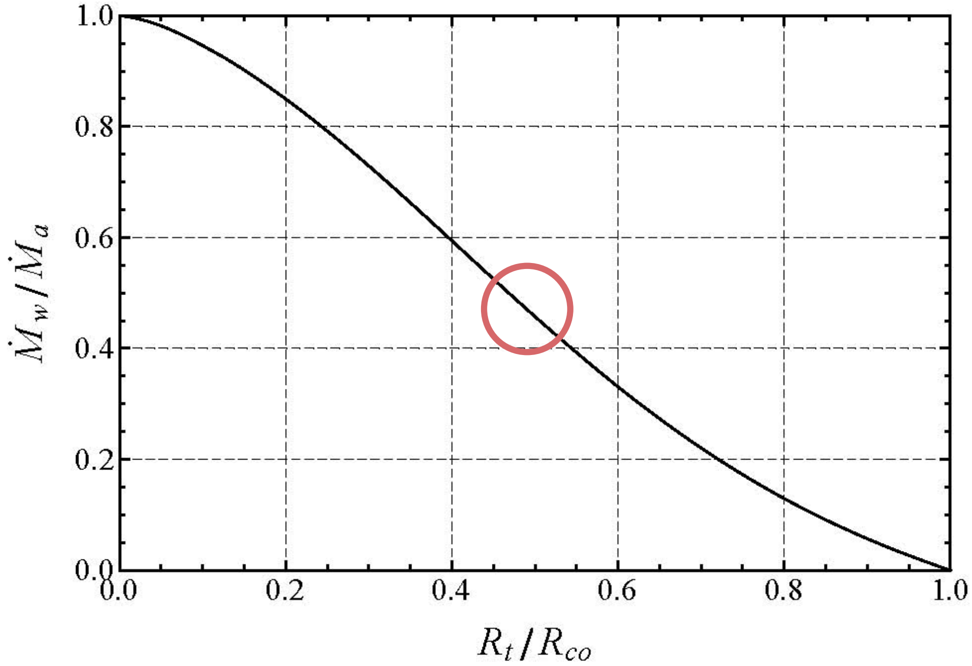

Mass ejection rate and speed
increases as
the inner edge approaches the star

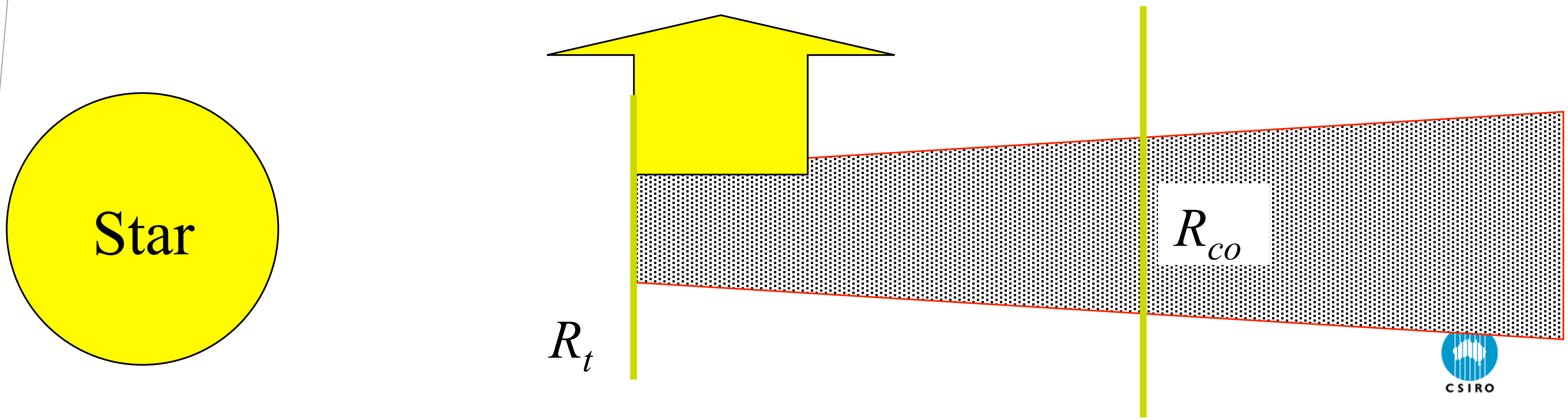

Predictions

Mass ejection is proportional to mass accretion

$$\dot{M}_w = \frac{\dot{M}_a}{4}\left(\left(\frac{R_o}{R_t}\right)^2 - 1\right)$$

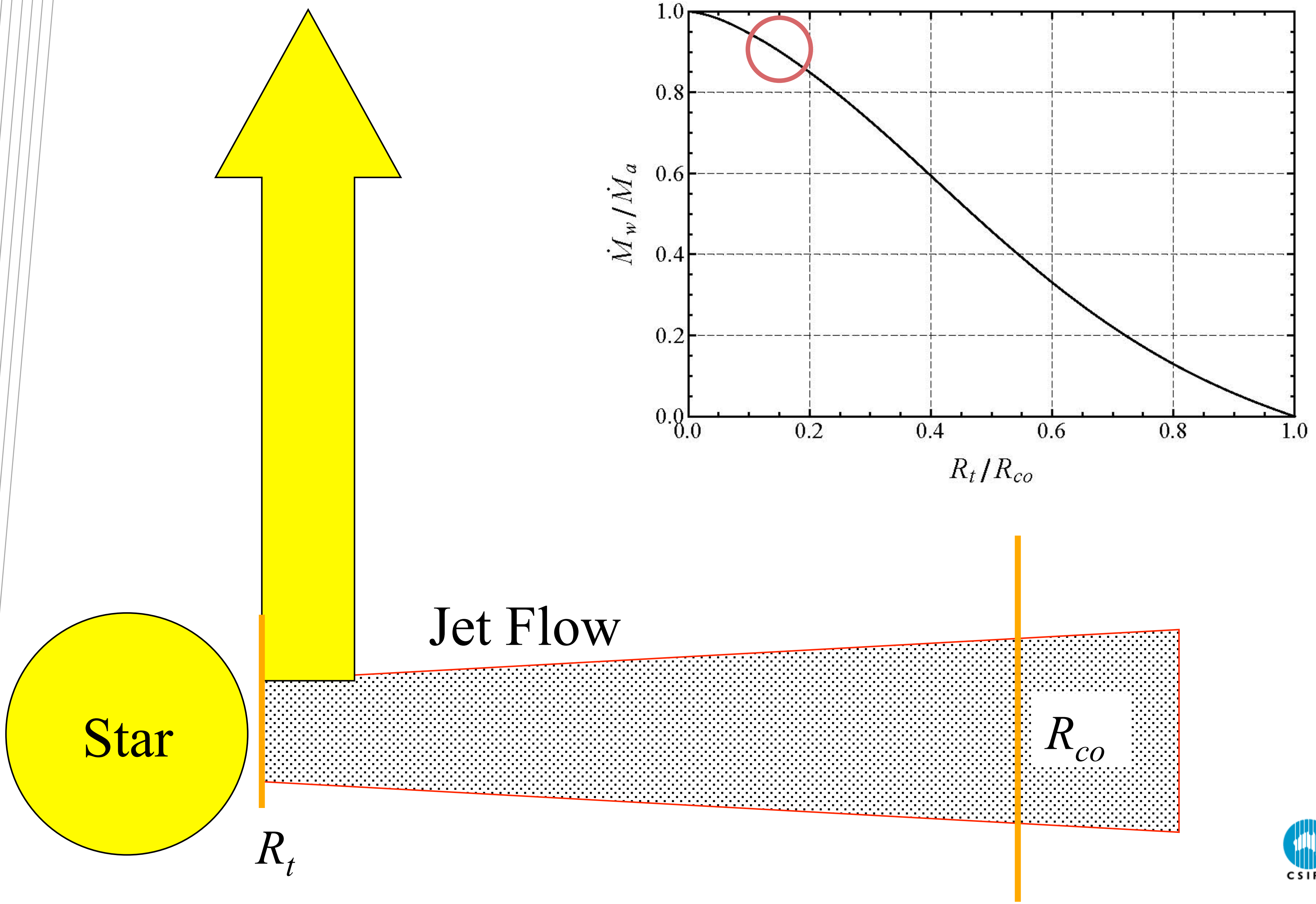

Laboratory Magnetic Jet Flows

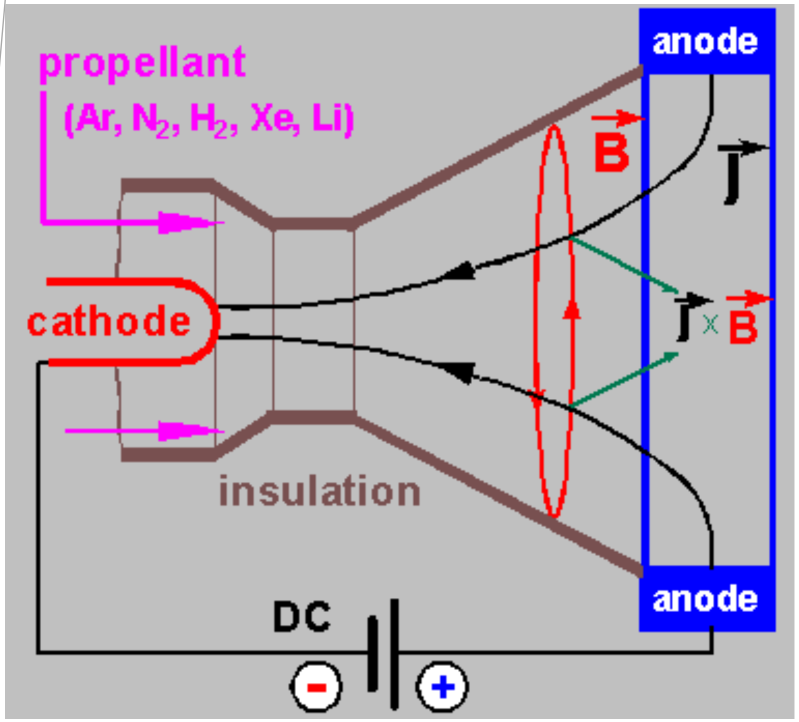

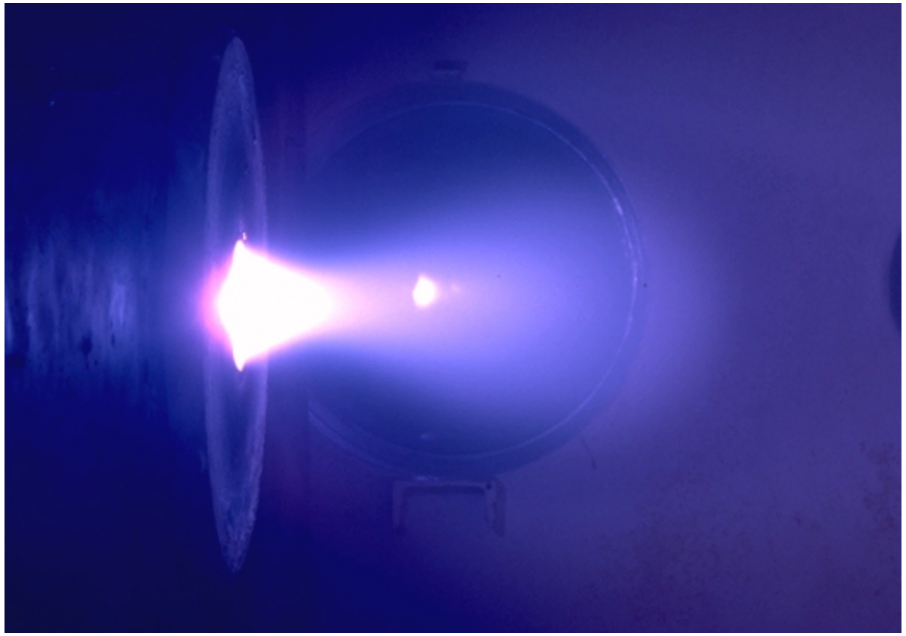

Fastest speed listed in the literature ~ 200 km/s

CSIRO

Professor Aleksej Ivanovich Morozov

Conclusions

(1) Much of the solid material in the solar accretion disk underwent thermal processing with radial transport

(2) A solar bipolar jet flow/rim wind could have provided the formation and transport mechanism for this material

(3) Mass ejection is proportional to mass accretion

(4) Toroidal fields may power the jet flows.

(5) Jet flows produced at the inner rim of the disk

(6) Mass ejection rate increases as the inner edge of the disk approaches the star and decreases as the inner edge approaches the co-rotation radius

(7) Inner disk is compressed by the jet flow

Meteorites may offer a way of deducing the mechanism for magnetically-driven outflows

CSIRO

CSIRO Material Science and Engineering
Kurt LIffman
Research Group Leader

Phone: 03 9252 6167
Email: Kurt.Liffman@csiro.au

www.csiro.au

Thank you

Contact Us
Phone: 1300 363 400 or +61 3 9545 2176
Email: enquiries@csiro.au Web: www.csiro.au

CSIRO

MHD Equations

$$\frac{\partial \rho}{\partial t} + \nabla \cdot (\rho \mathbf{v}) = 0$$

Mass Conservation

$$\frac{\partial \left(\rho \mathbf{v} + \varepsilon_0 \mathbf{E} \times \mathbf{B}\right)}{\partial t} + \nabla \cdot \left(\tilde{\mathbf{P}} + \rho \mathbf{v}\mathbf{v} - \tilde{\mathbf{M}}\right) = 0$$

Momentum Conservation

$$\tilde{\mathbf{M}} = \frac{\mathbf{B}\mathbf{B}}{\mu_0} + \varepsilon_0 \mathbf{E}\mathbf{E} - \tilde{\mathbf{1}}\left(\frac{\varepsilon_0 E^2}{2} + \frac{B^2}{2\mu_0}\right)$$

Maxwell Stress Tensor

$$\frac{\partial \left(u + \frac{1}{2}\rho v^2 + \frac{1}{2}\varepsilon_0 E^2 + \frac{B}{2\mu_0}\right)}{\partial t} + \nabla \cdot \left(\Phi_{ch} + \mathbf{v}\left(u + \frac{1}{2}\rho v^2\right) + \mathbf{v} \cdot \tilde{\mathbf{P}} + \frac{1}{\mu_0}\mathbf{E} \times \mathbf{B}\right) = 0$$

Energy Conservation

$$u = \frac{p}{\Gamma - 1}$$

Equation of State

$$j = \sigma\left(\mathbf{E} + \mathbf{v} \times \mathbf{B}\right)$$

Ohm's Law

And Maxwell's Equations

Energy Conservation

We want the conservative form:
which $\Rightarrow Q$ is a flow constant

$$\nabla \cdot (\mathbf{v}Q) = 0$$

Steady state
isotropic pressure

$$\nabla \cdot \left(\mathbf{v}\left(\boldsymbol{u} + \frac{1}{2}\rho \boldsymbol{v}^2 + \boldsymbol{p} \right) + \frac{1}{\mu_0}\mathbf{E}\times\mathbf{B} \right) = 0$$

$$+$$

Infinite conductivity

$$\mathbf{E} + \mathbf{v}\times\mathbf{B} = 0$$

$$+$$

Equation of State

$$u = \frac{p}{\Gamma - 1}$$

$$\Downarrow$$

$$\nabla \cdot \left(\mathbf{v}\left(\boldsymbol{u} + \frac{1}{2}\rho \boldsymbol{v}^2 + \boldsymbol{p} + \frac{\boldsymbol{B}^2}{\mu_0} \right) - \frac{\mathbf{B}}{\mu_0}\mathbf{v}\cdot\mathbf{B} \right) = 0$$

V || B

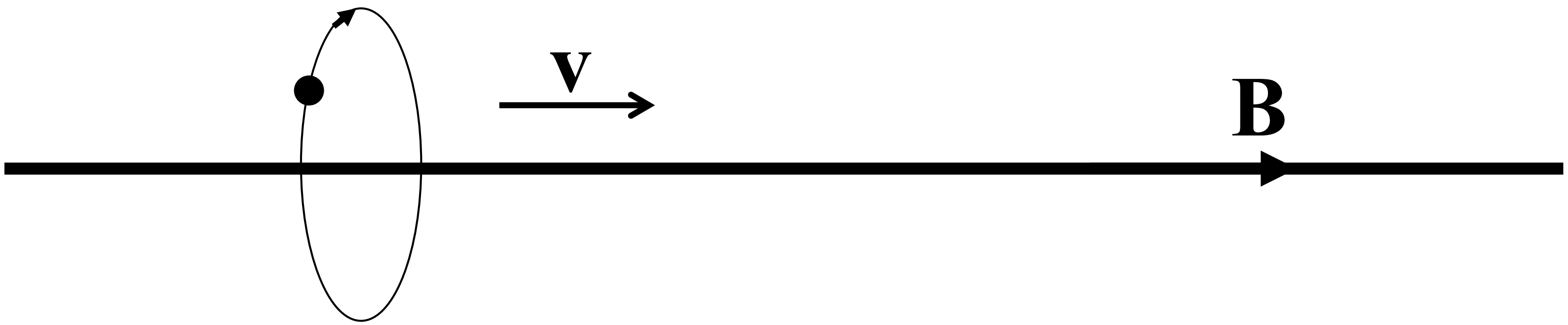

$$\nabla\cdot\left(\mathbf{v}\left(\boldsymbol{u}+\frac{1}{2}\rho\boldsymbol{v}^2+\boldsymbol{p}\right)\right)=0 \qquad + \text{ other flow constants}$$

$$\Downarrow$$

$$\left(\left(\frac{v}{C_s}\right)^2-1\right)\frac{dv}{v}=\frac{dA}{A} \quad \text{where} \quad C_s^2=\frac{\Gamma p}{\rho}$$

De Laval Nozzle Equation

Converging/Diverging Nozzle

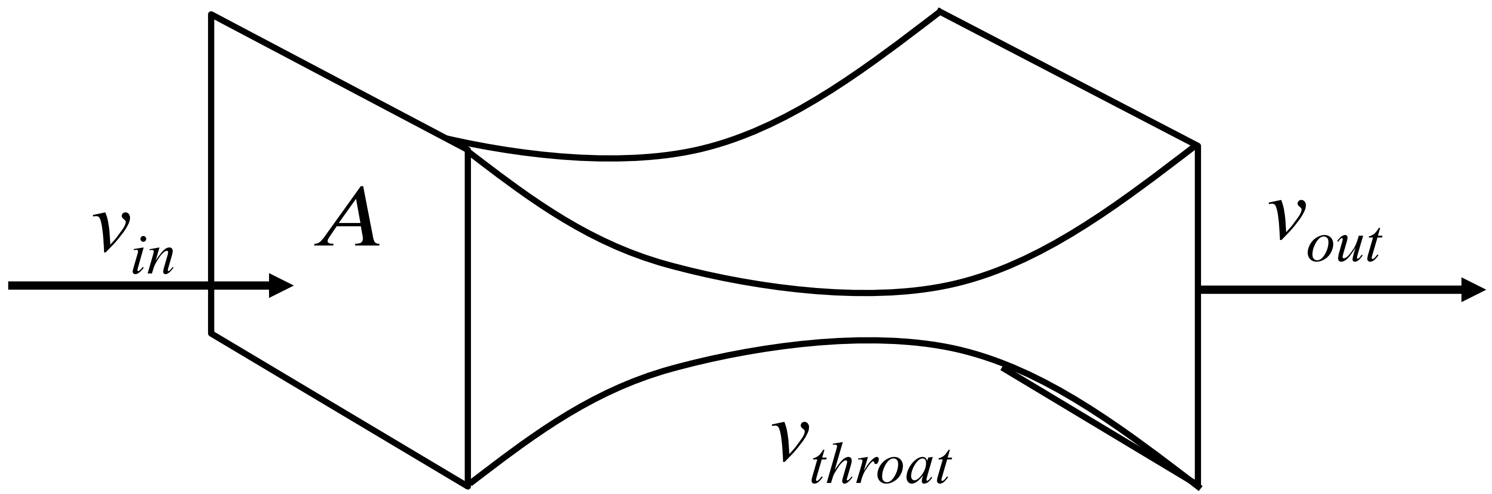

$$\left(\left(\frac{v}{C_s}\right)^2 - 1\right)\frac{dv}{v} = \frac{dA}{A}$$

$$v \approx 0,\ dv > 0, \Rightarrow\ dA < 0;$$
$$v = C_s,\ dv > 0, \Rightarrow\ dA = 0;$$
$$v > C_s,\ dv > 0, \Rightarrow\ dA > 0.$$

V ⊥ B

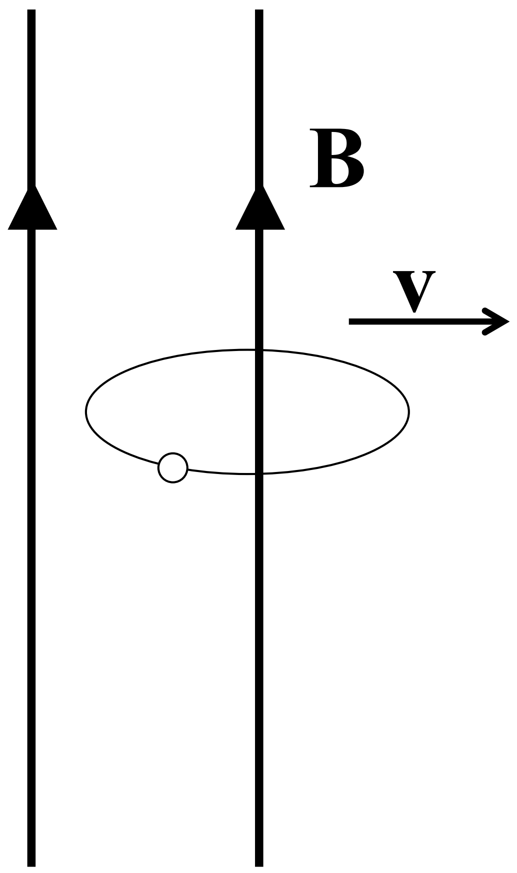

$$\nabla \cdot \left(\mathbf{v} \left(u + \frac{1}{2}\rho v^2 + p + \frac{B^2}{\mu_0} \right) - \frac{\mathbf{B}}{\mu_0} \mathbf{v} \cdot \mathbf{B} \right) = 0$$

$$\Downarrow$$

$$\nabla \cdot \left(\mathbf{v} \left(u + \frac{1}{2}\rho v^2 + p + \frac{B^2}{\mu_0} \right) \right) = 0$$

$$\Downarrow$$

$$\left(\left(\frac{v}{C_F} \right)^2 - 1 \right) \frac{dv}{v} = \frac{dA}{A}$$

Magnetic Nozzle

where

$$C_F^2 = C_A^2 + C_S^2$$

Fast Magnetosonic Speed

$$C_A^2 = \frac{B^2}{\mu_0 \rho}$$

Alfvén Speed

C_A and C_S

$$C_S = 11.8\left(\frac{T}{10^4\ \mathrm{K}}\right)^{1/2}\ \mathrm{km\,s^{-1}}$$

and

$$C_A = 282\left(\frac{B}{100\,\mathrm{G}}\right)\left(\frac{\rho}{10^{-12}\ \mathrm{g\,cm^{-3}}}\right)^{-1/2}\ \mathrm{km\,s^{-1}}$$

So there exists the possibility of high speed flow, relatively low temperature flow in a magnetic jet.

Radial Transport of Processed Material in Circumstellar Disks

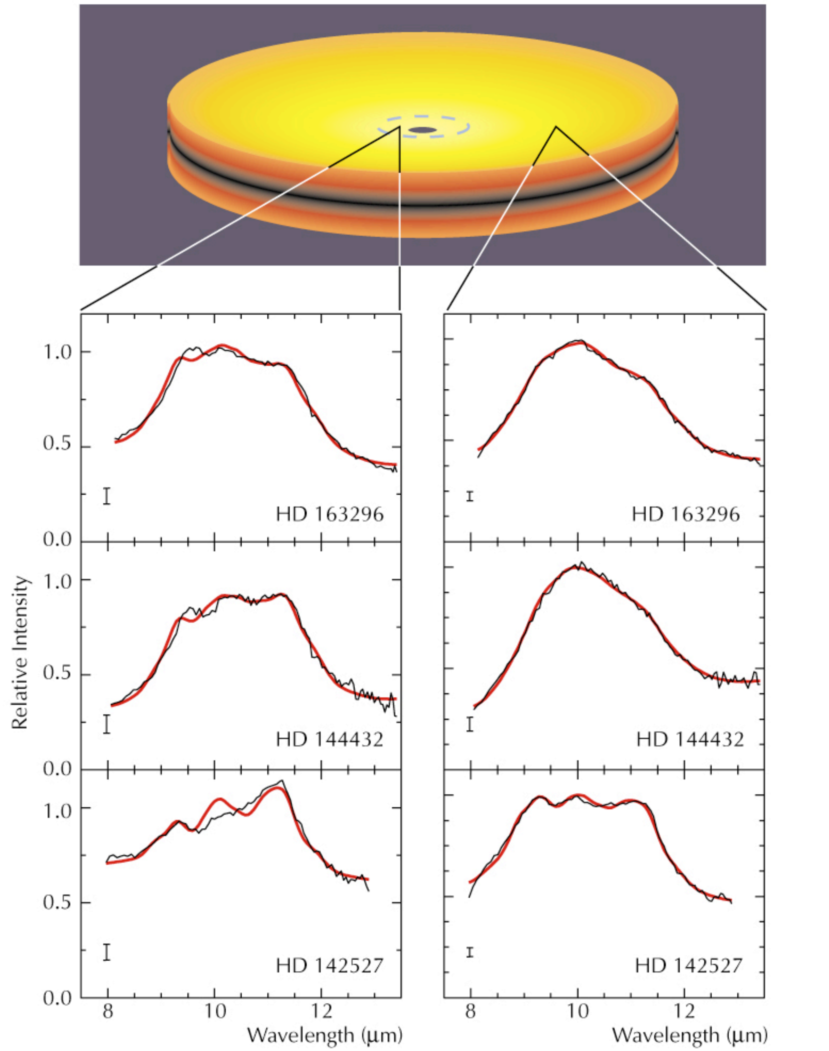

Mid-IR Spectra of Inner and Outer Discs Around Three Young Stars

Van Boekell *et al*. 2004

The dust in the ISM has an amorphous structure.

Inner disk dust ~ 90% crystalline silicate.
Outer disk dust ~40% crystalline silicate

The dust in inner disks is more processed. Evidence suggests that the dust is processed in the centre of the disk and then moves radially outwards.

Transport mechanisms from the inner to outer sections of the accretion disk

transport mechanism from the inner to outer regions of YSO accretion disks

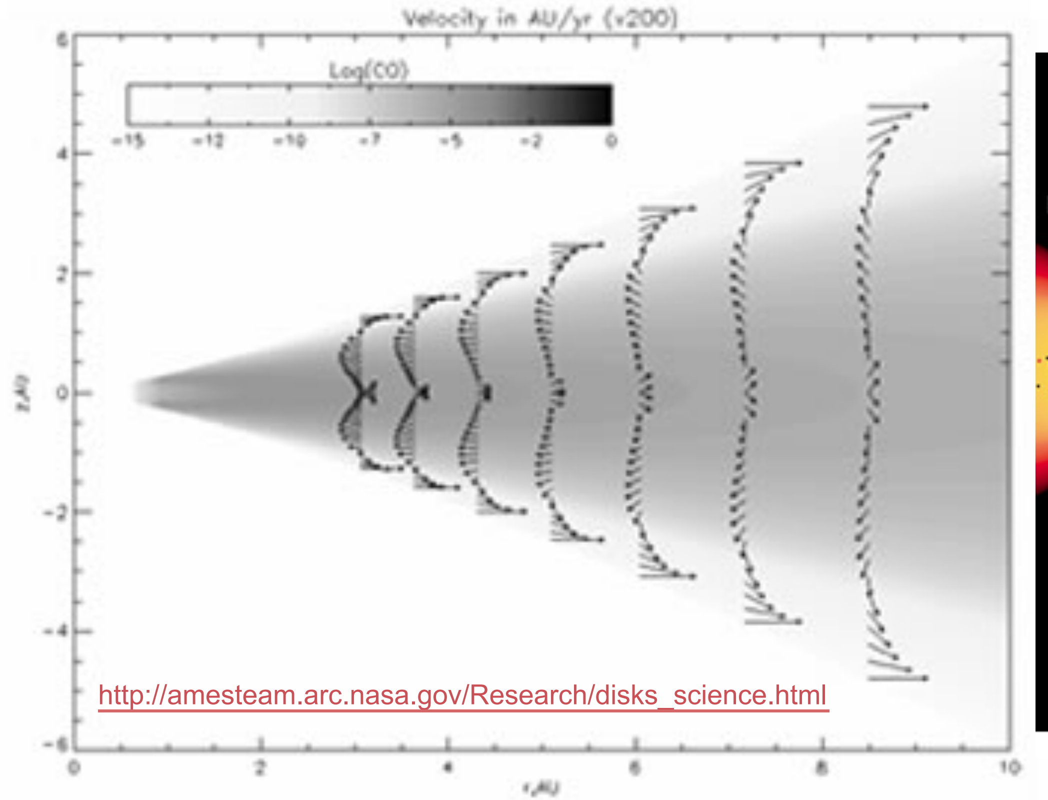

Figure 2. Velocity vectors obtained from the dynamical equations showing variation in vertical and horizontal directions. The shading indicates abundances of CO gas based on chemical network calculations.

Turbulent Eddy Advection (Morfill and Volk 1984)

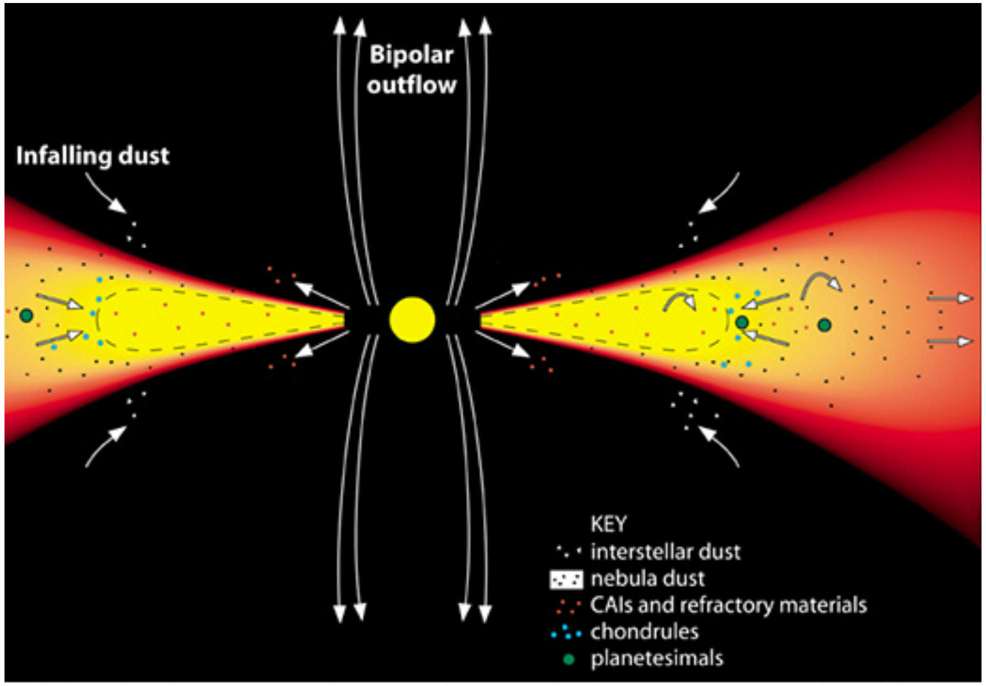

(PSRD graphic by Nancy Hulbirt, based on a conceptual drawing by Edward Scott, Univ. of Hawaii.)

Outflow Transport
(Skinner, Liffman, Shu &c)

CSIRO

Photo-evaporation and YSO disks

Photo-evaporation gives the gravitational radius: R_g ~ 1 AU (Liffman 2003)

Photoevaporation splits the disk into an inner and outer disk (Gorti et al 2009)

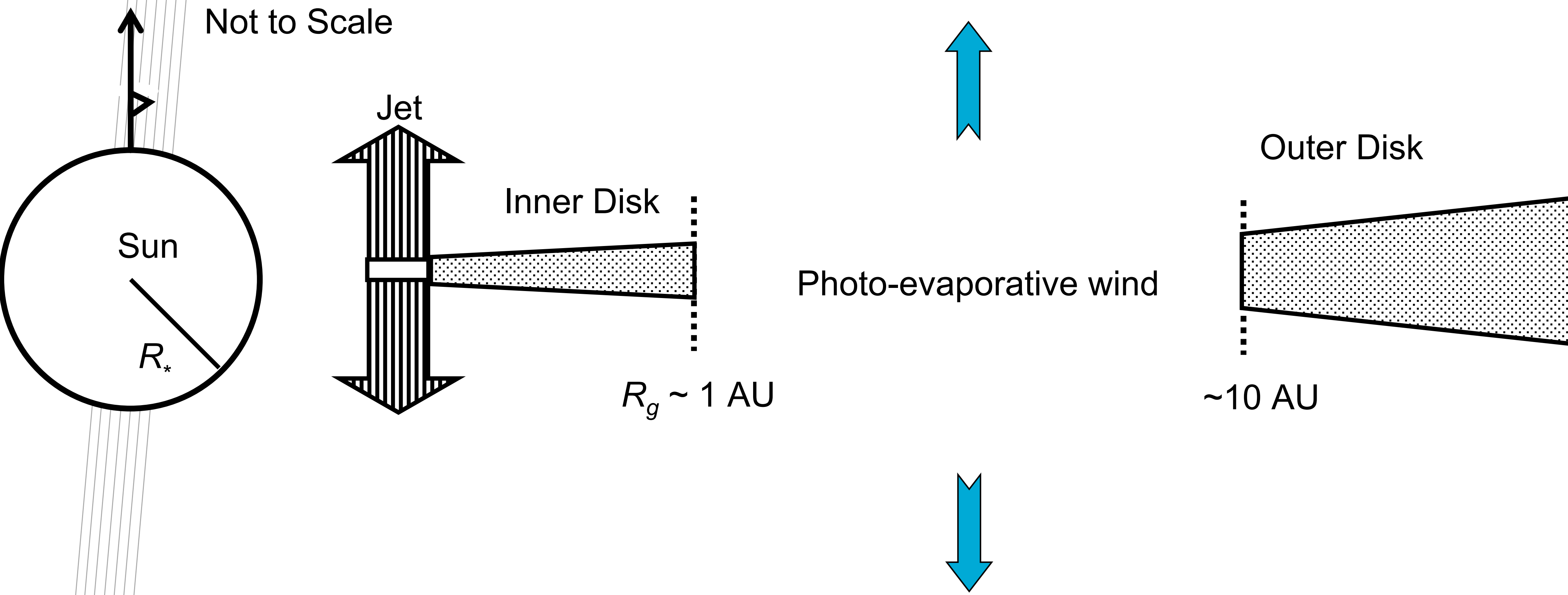

If there is not disk then turbulent convective transfer might have a problem